Graphic design: Communication Division, UiB / Print: Skipnes Kommunikasjon AS

uib.no

ISBN: 978-82-308-3847-1

2018 Low Salinity Surfactant Flooding in Sandstone Cores • Annette Meland Johannessen

Low Salinity Surfactant Flooding in Sandstone Cores

Annette Meland Johannessen

Thesis for the Degree of Philosophiae Doctor (PhD)
University of Bergen, Norway
2018

UNIVERSITY OF BERGEN

Low Salinity Surfactant Flooding in Sandstone Cores

Annette Meland Johannessen

Thesis for the Degree of Philosophiae Doctor (PhD)
at the University of Bergen

2018

Date of defence: 26.01.2018

© Copyright Annette Meland Johannessen
The material in this publication is covered by the provisions of the Copyright Act.

Year: 2018
Title: Low Salinity Surfactant Flooding in Sandstone Cores

Name: Annette Meland Johannessen
Print: Skipnes Kommunikasjon / University of Bergen

Preface

This thesis is submitted for the degree of Philosophiae Doctor to the Department of Chemistry at the University of Bergen. It consists of three scientific papers along with an introduction to relevant topics. The papers are based on research work performed at the Centre for Integrated Petroleum Research (CIPR) at the University of Bergen in the period September 2010 to December 2013. The project was part of the PETROMAKS program initiated and sponsored by the Norwegian Research Council.

The thesis includes research on the hybrid EOR process of low salinity surfactant injection. The main objective was to investigate whether combining the two processes of low salinity injection with surfactant injection would be more efficient than either of the processes alone.

The first five chapters introduce the concept of surfactant flooding and the low salinity effect (LSE) and important aspects around these processes both alone and combined. A summary of the main results follows which are based on the results from the papers that are included at the end of this thesis.

Acknowledgements

I wish to express my gratitude to my supervisors Associate Professor Kristine Spildo and Professor Arne Skauge for giving me this opportunity and for shearing their knowledge with me. I will always be in debt to Kristine Spildo for her continuous support, guidance and encouraging words throughout these years.

I big thank you to all fellow students and colleagues at CIPR that I have met over the years, many of which I still consider as close friends.

A big thank you goes to a very special person, Bartek Vik, for his support and motivation on both a personal and professional level. I admire your always optimistic way of being which have helped me to keep things in perspective.

Last but not least I would like to thank the rest of my family and friends for all their support, motivation and for always having belief in me.

Abstract

A new generation enhanced oil recovery (EOR) methods comes from combining techniques to make the overall process more efficient than either of the processes alone. These combined methods are often called hybrid EOR methods, and in this work, we investigate the potential for further enhancement of oil recovery by combining low salinity (LS) and surfactant (S) injection.

When injecting LS water that holds a significantly lower salinity than the formation water salinity, it is believed that destabilization of oil layers adhering to mineral surfaces making the surface more water-wet could be a contributing mechanism to EOR.

Surfactant flooding is a proven EOR technique, which mobilizes capillary trapped oil by lowering the oil water Interfacial Tension (IFT). The majority of the literature on the topics of low salinity and surfactant flooding addresses one or the other. In this study, however, we investigated whether combining the two processes of low salinity injection with surfactant (LSS) injection would be more efficient than either of them applied alone. We propose that by taking advantage of the oil that has been destabilized by LS injection, only a moderate reduction in IFT by adding surfactant could contribute to production of the destabilized oil, which may not reach the producer if capillary forces are high.

We showed that by taking advantage of the oil destabilized by LS injection, and combining it with Winsor I surfactant flooding experiments to give a moderate reduction in IFT, the combined process gave comparable recoveries to traditional surfactant flooding experiments operating in the ultralow IFT regime.

Further, comparing data from LSS experiments to high salinity surfactant (HSS) injection experiments at similar capillary numbers showed lower residual oil saturations for the LSS experiments. The different CDC for LSS experiments indicate that there is a combined effect of IFT reduction and LS injection on oil recovery compared to a traditional reduction in IFT alone.

List of publications

Paper I	Spildo, K., Johannessen, A., M. and Skauge, A. (2012) *Low Salinity Waterflood at Reduced Capillarity.* SPE-154236. Presented at the Eighteenth SPE Improved Oil Recovery Symposium, April 14-18, Tulsa, Oklahoma.
Paper II	Johannessen, A., M. and Spildo, K. (2013) *Enhanced Oil Recovery (EOR) by Combining Surfactant with Low Salinity Injection.* Published in Energy & Fuels, 27, 10: 5738-5749.
Paper III	Johannessen, A., M. and Spildo, K. (2014) *Can Lowering the Injection Brine Salinity Further Increase Oil Recovery by Surfactant Injection under Otherwise Similar Conditions?* Published in Energy & Fuels, 28, 11: 6723-6734.

Abbreviations and Symbols

A	Area
APS	Alcohol Propoxy Sulfate
C	Empiric constant
CDC	Capillary Desaturation Curve
c_i	Molality of element *i*
CMC	Critical Micelle Concentration
COBR	Crude Oil/Brine/Rock
C_{SC}	Critical Salt Concentration
DLVO-theory	Derjaguin-Landau-Verwey-Overbeek-theory
dP	Differential Pressure
EDS	Energy Dispersive Spectroscopy
EOR	Enhanced Oil Recovery
G	Free energy
HS	High Salinity
HSS	High Salinity Surfactant
I	Ionic strength
IAA	Isoamyl Alcohol
I_{AH}	Amott Harvey wettability index
IFT	Interfacial Tension
I_O	Wettability index to oil
IOS	Internal Olefin Sulfonate
I_{Swi}	Intensity at S_{wi}
$\bar{I}_{Swi}$	Average intensity at S_{wi}
I_W	Wettability index to water
$I_{100\%\ water}$	Intensity at 100% water saturation
$\bar{I}_{100\%\ water}$	Average intensity at 100% water saturation
K	Absolute Permeability
k_{ri}	Relative Permeability to phase i
LS	Low Salinity
LSE	Low Salinity Effect
LSS	Low Salinity Surfactant
LSWAG	Low Salinity Water Alternating Gas
MIE	Multicomponent Ion Exchange
N_c	Capillary Number
N_{cc}	Critical Capillary Number
OOIP	Originally Oil In Place
OS	Optimal Salinity
OSS	Optimal Salinity Surfactant
ΔP	Pressure difference
R	Radius of curvature
S^*	Optimal Salinity
SBA	Secondary Butanol Alcohol
S_O	Oil saturation
S_{or}	Residual oil saturation
S_{orc}	Residual oil saturation after a chemical flood
$S_{or,LS}$	Residual oil saturation after LS injection
$S_{or,LSS}$	Residual oil saturation after LSS injection
S_{orw}	Residual oil saturation after waterflood
$S_{o,Swi}$	Oil saturation at S_{wi}
$\bar{S}_{o,S_{wi}}$	Average oil saturation at S_{wi}
SP^*	Solubilization parameter at optimal salinity
SP_i	Solubilization parameter for phase i
STO A	Stock tank crude oil A
STO B	Stock tank crude oil B

SW	Seawater
S_w	Water saturation
S_{wi}	Irredusible water saturation
S13	Isotridecyl alchol 13PO sulphate
ΔS_{wf}	Forced change in water saturation
ΔS_{ws}	Spontaneous change in water saturation
v	Darcy velosity
V_i	Volume of phase i
V_s	Volume of surfactant
WAG	Water Alternating Gas
WBT	Water BreakThrough
Winsor I	Lower Phase Microemulsion
Winsor II	Upper Phase Microemulsion
Winsor III	Middle Phase Microemulsion
WOR	Water Oil Ratio
z_i	Charge of element *i*
μ	Viscosity
σ	Interfacial Tension

Contents

PAPERS

1. INTRODUCTION

Predictions of world energy consumption in the coming years are associated with high uncertainties. However, one thing is certain; the energy consumption is going to grow. Renewable energy sources are expected to play a bigger part in the energy supply than earlier, both to close the gap between energy supply and demand, but also due to climate challenges and global agreements on climate goals. The energy landscape will thus undergo adjustments with mixed energy supplies from both renewables and fossil energy. Nevertheless; fossil fuels will still remain as the bedrock of global energy. The energy systems are expected to increase in complexity, both across and within technologies, to improve efficiencies meeting the high energy demand. The oil industry has observed the transition in the energy market and moves towards new strategies ensuring higher recovery factors [1,2].

Over half of the oil originally in place (OOIP) may be trapped in the reservoir after a conventional sea water (SW) flooding due to dominating capillary forces and/or poor sweep efficiency. This oil is the target for Enhanced Oil Recovery (EOR) methods and the potential to extend the reservoir's lifetime, and thereby contribute on narrowing in on the energy gap. To enhance the oil recovery efficiency further, there have been growing focuses lately on developing recovery methods that combine different EOR methods – so called hybrid methods.

The displacement of oil by injection of unlimited accessible sea water has traditionally been understood as a physical process where water maintains reservoir pressure simultaneously as mobile oil is swept towards a producing well. Studies conducted during the past decade however, have concluded that oil recovery by waterflooding also involves chemical processes between the Crude Oil, Brine and Rock (COBR). Introducing injection water with a significantly lower ionic strength than that of the connate water can therefore contribute to increased recovery beyond the classical secondary SW recovery, which is called the Low Salinity Effect (LSE). Although the dominating mechanism(s) behind the LSE is not fully understood a frequent observation in the porous media after a Low Salinity (LS) injection process is a wettability shift going from less to more water-wet state. Thus, the LSE can be summarized as destabilization and mobilization of oil layers adsorbed or adhered to rock minerals. Speculations have been made whether the LS injection often show no, or moderate effect due to the absence of a continuous oil film.

The aim of a surfactant flooding is to decrease the water-oil Interfacial Tension (IFT) and capillary forces in the porous media and thereby increase the microscopic sweep to reduce the residual oil. Optimised surfactant systems showing ultralow water-oil IFT have in theory a high efficiency on oil recovery, but it is often proven difficult to design and manufacture specialized, yet cost-effective, surfactant systems needed for applications at high salinities. Surfactant flooding in a LS environment on the other hand, opens up for using a wider range and more commercially available low-cost surfactant systems. The drawback is that their IFT properties often are higher than in high salinity environments resulting in lower oil recovery efficiency. This compromise has led to the investigation of the hybrid EOR method of Low Salinity Surfactant (LSS); the surfactant takes advantage of the destabilised oil in a LS regime resulting in a combined process which is more efficient than either of the processes alone.

This thesis focuses on surfactant flooding in a LS environment. The main objective has been to investigate whether LS flooding in the presence of surfactant could be an attractive EOR technique compared to LS or surfactant flooding applied alone.

The hypothesis is that oil layers destabilized by LS flooding can be trapped before they are produced. Traditional surfactant flooding at ultralow IFT yields very high recoveries, however, it is usually associated with high cost. Surfactant systems in LS environments are easier to control at lower costs than traditional surfactant systems. The drawback is that these systems tend to show higher water-oil IFT than traditional systems. Combining the techniques of LS and surfactant flooding takes advantage of the destabilized oil by LS injection and with only a moderate reduction in IFT by surfactant flooding can mobilize the destabilized oil and/or reduce the trapping of mobilized oil.

2. WATERFLOODING AND ENHANCED OIL RECOVERY (EOR)

Traditional methods of oil recovery through primary and secondary methods only recover between a quarter and half of the oil reserves present in the reservoir. In order to extend the economic lifetime of oil reservoirs the remaining oil is a target for tertiary oil recovery methods, or EOR methods, by improving the microscopic and/or volumetric displacement efficiency.

The definition of EOR is often linked to the use of unconventional recovery methods. Sometimes EOR is defined as oil recovery by injection of materials usually not present in the reservoir such as e.g. surfactants and polymers. Even though injection of low salinity (LS) water falls outside the strict definition of EOR, it is an unconventional technique that is defined as an EOR method.

2.1 Waterflooding

Waterflooding is a method of secondary recovery in which water (most often sea water) is injected into the reservoir formation to displace residual oil. It can follow primary recovery where the reservoir's natural energy (fluid and rock expansion, solution gas drive, gravity drainage and aquifer influx) is used as drive mechanisms to produce oil. The principal reason for performing a waterflood is to increase oil recovery which is accomplished by voidage replacement where water push and replace oil towards production wells.

Waterflooding is the most commonly used secondary oil recovery method because of its relatively simple technology, it is inexpensive, readily available in large volumes, and especially because water can effectively increase oil recovery substantially [3].

2.2 Surfactant flooding

The use of surfactants as a tertiary oil recovery method, or EOR method, has been recognised since the early 1930's [4]. Surfactant flooding is the process where surface active materials are added to the injection fluid to reduce the Interfacial Tension (IFT) to oil and mobilise and displace residual oil.

Traditionally, surfactant floods are carried out in the Winsor III region due to the ultralow IFT and excellent oil displacement, see chapter 3.1.2. However, the design of these surfactant floods can be challenging and expensive [5,6] since the Winsor III region often appears at a narrow salinity window which can be difficult to maintain, and the surfactant flood can degenerate due to surfactant dilution, dispersion, adsorption onto the rock surface or precipitation of surfactant by high salinity reservoir brine.

An alternative is to perform the surfactant flood in the Winsor I region at lower salinity environments. These systems are believed to be easier to control than a flood in the Winsor III region, because they are expected to be less sensitive to changes in reservoir conditions and surfactant concentrations and the retention is generally lower at these salinity conditions. Flooding operations in low salinity environments opens up to a wider range of commercially available, low-cost surfactant systems The drawback of this design is that the moderate reduction in IFT are usually not low enough for good oil displacement [5].

2.3 Capillary Desaturation Curve (CDC)

On a microscopic level, capillary forces are, in part, responsible for the inefficiency during displacement of oil by waterflooding. As the displacement of oil by water proceeds, the oil phase eventually disintegrates into blobs of residual oil (S_{or}). The trapped oil can be recovered by the use of EOR methods, by either reducing the capillary forces, whose strength is set by the oil/water interfacial tension, or by the viscous forces acting on the trapped phase to exceed the capillary retaining forces [4,7-11]. The relationship between these forces and S_{or} can be described by the dimensionless capillary number, N_c

$$N_c = \frac{\mu v}{\sigma} \tag{2.1}$$

where the μ is the viscosity of displacing fluid, v is the Darcy velocity of the displacing fluid and σ is the IFT between the oil and the displacing fluid.

The capillary desaturation curve (CDC) shows the relationship between N_c and $S_{or,}$ (Figure 2.1), and the shape of the curve depends on type of rock, pore size distribution and wettability [12].

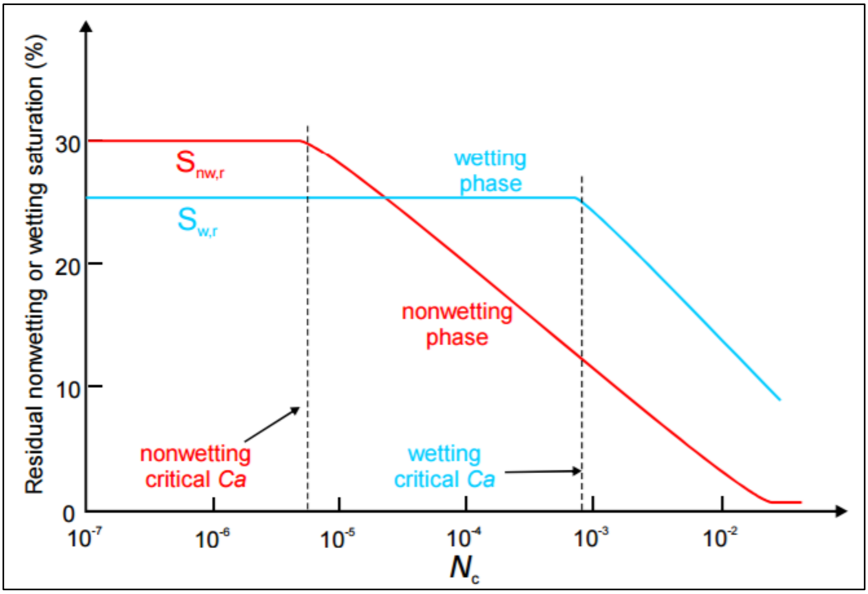

Figure 2.1 – CDC curve showing S_{or} of the wetting and non-wetting phase as function of the N_c. Taken from [13].

At low N_c the CDC remains constant which represent the lowest achievable S_{or} by for example SW flooding. The N_c required to decrease S_{or} below the plateau is called the critical capillary number (N_{cc}), In order for the N_c to increase according to equation (2.1) and thus the S_{or} to decrease according to Figure 2.1, either the displacement flow rate must increase, the displacing fluid viscosity must increase (e.g. by polymer) and/or the IFT between oil and displacing fluid must decrease (e.g by surfactant).

2.4 Hybrid EOR processes

Research on combining methods and processes in the energy sector have recently become more attractive due to increased focus on energy and production efficiency from both an economic and environmental perspective.

On the EOR side, studies combining low salinity (LS) injection with other well-known EOR processes have increased lately. LS water combined with polymer flooding have proven an efficient EOR process due to lower polymer retention and a lower polymer concentration is required to obtain the same target viscosity as in a high salinity environment [14,15].

LS water combined with CO_2water-alternating-gas (WAG) has also shown promising results compared to the processes alone. CO_2 (LSWAG) injection promotes the synergy of the mechanisms underlying these methods to further enhance oil recovery and overcome late-production problems frequently encountered in conventional WAG [16].

3. SURFACTANTS AND PHASE BEHAVIOR

Surfactants, or **surf**ace **act**ive **a**ge**nts**, refer to a group of molecules that have a tendency to adsorb at interfaces between two immiscible phases, and thus reduce the Interfacial Tension (IFT) between the fluids. It is the amphiphilic structure, i.e. their hydrophilic (polar) and hydrophobic (non-polar) moieties, that gives these molecules their adsorbing characteristics [17]. Another important characteristic of surfactants is that they have an ability to form self-assembled structures in aqueous solution, called micelles. Micelle structures spontaneously formed by surfactants in solution are created to reduce the exposure of the hydrocarbon chains to water and thereby reduce the free energy of the system. One of the most important consequences of the micellization phenomenon is that the micelles provide a non-polar environment within the aqueous medium. In addition to the formation of micelles that greatly enhance the solubility of the surfactant itself beyond what would be if micelles did not form, the solubility of other less soluble organic materials is greatly enhanced as well [17].

Surfactants are classified into four main groups according to their polar moieties which are anionic, cationic, non-ionic and amphoteric surfactants. Anionic surfactants are the most commonly surfactant group used in EOR applications. In addition to their nature of a negatively charged head group which show a low adsorption level compared to other surfactant groups, they efficiently reduce interfacial tension (IFT) and they are relatively inexpensive to produce.

3.1 Microemulsion phase behavior

Schulman and co-workers [18] introduced the term “micro emulsion”, and Healy and Reed [19] defined the term microemulsion further to be a stable, translucent micellar solution of oil, water that may contain electrolytes, and one or more amphiphilic compound (e.g. surfactants and/or alcohols) [19]. Winsor [20] classified oil/water/surfactant microemulsions as Winsor I, Winsor II and Winsor III. A transition in microemulsion phase behavior is caused by different variables; see 3.1.1, which is often studied through ternary phase diagrams [17,19,21]. Each corner represents at least one component – surfactant, water/brine and oil, but often are pseudo-components like co-solvent included in one of the components.

For simple systems, the ternary diagram divides into two or four regions. In each case, every compositional point within the single-phase region above the binodal curve corresponds to a microemulsion. Compositional points below the binodal point correspond to multiple phases, comprising, in general, microemulsions, excess oil and excess water.

Figure 3.1 a) below shows a two-phase region where an excess oil phase exists in equilibrium with the microemulsion phase, Winsor I. Such systems are often also called II- systems where II indicates that no more than two phases can form, and – refers to the negative slope of the tie lines, i.e. lower phase microemulsion.

Figure 3.1 b) show a Winsor II (or II+) microemulsion system where water-in-oil microemulsion is in equilibrium with an excess water phase. The water or brine is solubilized through the formation of swollen micelles with brine located in the core of the micelles.

A third surfactant rich phase can form within the three-phase region, Figure 3.1 c), which separates into excess oil, excess brine and a microemulsion phase which contain both oil and water, Winsor III.

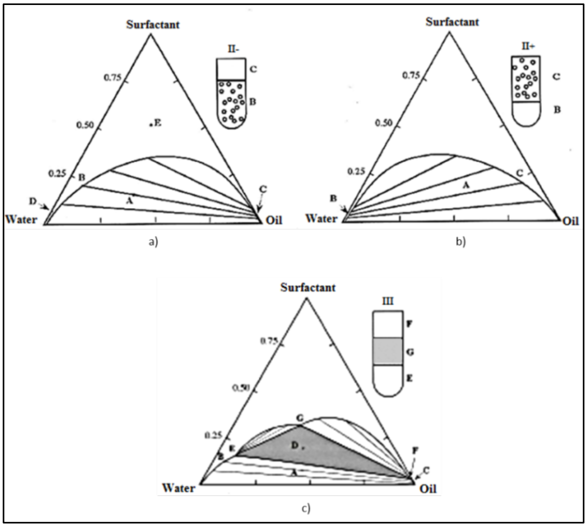

Figure 3.1 – Ternary diagrams, containing water, oil and surfactant, showing the phase behavior of three different microemulsion systems: a) Winsor I system, b) Winsor II system, and c) Winsor III system [22].

3.1.1 Influence on phase behavior

Variations in one or several parameters included in a microemulsion system, such as salinity, temperature, co-solvent, surfactant concentration, WOR, type of oil, can cause a transition in the microemulsion phase behavior. Knowledge on how the parameters affect the phase behavior is important when developing and optimizing a surfactant system satisfying specific flooding criteria [23].

The effect of increasing salinity is shown by the ternary diagrams in Figure 3.1. In these multicomponent systems salt is assumed to be included in the water component [24]. A gradual increase leads to a Winsor I > III > II phase transition, and is a classical phase behavior scan for surfactant flooding studies.

Alcohol, often termed co-solvent, is usually added to surfactant systems to help surfactant solubility and reduce equilibration time. This is achieved when alcohol molecules partition between the aqueous and oleic phases and the amphiphilic film, by decreasing the interfacial layers rigidity [25].

However; the addition of alcohol can compromise the reduction in IFT, thus reducing the solubilization parameters [26].

Co surfactants are also used to enhance the solubility of the system, but can also be used to tailor the system to e.g. a specific salinity.

There are no general trends when the surfactant concentration is varied in phase behavior studies. Variations in surfactant concentration was investigated by Healy et al. [21] which claim that if the overall surfactant concentration of the samples is changed, the phase diagram will change, reflecting the multicomponent nature of surfactant, co-solvent, brine and oil used. Wade et al. observed that the magnitude of variation of optimal conditions with surfactant concentration decreases as surfactant purity increases [27]. At low surfactant concentrations, the intermediate Winsor III system may not be observed. Instead a direct Winsor I ↔ II is found that is characterized by a minimum in IFT [23].

The literature also reports contradictory phase behavior results when the effect of varying WOR is investigated. Phase transition of Winsor I < III < II as the WOR increases was found by Healy et al. [21], and agrees with the WOR study in P2 [28] in this thesis. In contrast, a Winsor I > III > II phase transition was found by Tien and Bettahar [29], and practically no variation was found by Flaaten et al. [6].

Salager et al. [23] summarized the effect of systematically increasing several variables, including surfactant concentration and WOR, on the phase behavior of anionic surfactants. No systematic phase behavior transitions were observed on these two scans, thus concluding that the effect of varying the surfactant concentration or WOR is complex and dependent on the specific system. Contradictory effects on phase behavior when varying surfactant concentration and WOR reflect the importance of the initial phase behavior screening procedure.

3.1.2 IFT and Phase Behavior

The interfacial tension (IFT) is the amount of energy required to increase the surface of a liquid by a unit area [30], and can be given by equation (3.1)

$$\sigma = \frac{dG}{dA_G} \tag{3.1}$$

where σ is the surface/interfacial tension, G is the free energy and A is the area.

The work done in this process can be measured, for example by the spinning drop method (chapter 5.3), and the value of the IFT can be obtained.

A closer look at the test tube from the Winsor III region in Figure 3.1 c), reveal that two kinds of interfaces are present and therefore up to three interfacial tensions (IFT) can be measured. These are between microemulsion and excess water, **G** and **E**, microemulsion and excess oil, **G** and **F**, and excess water and excess oil, **E** and **F**.

Healy et al. [21] originally proposed the relation between phase behavior and IFT (Figure 3.2) which later was theoretically supported by Huh [31].

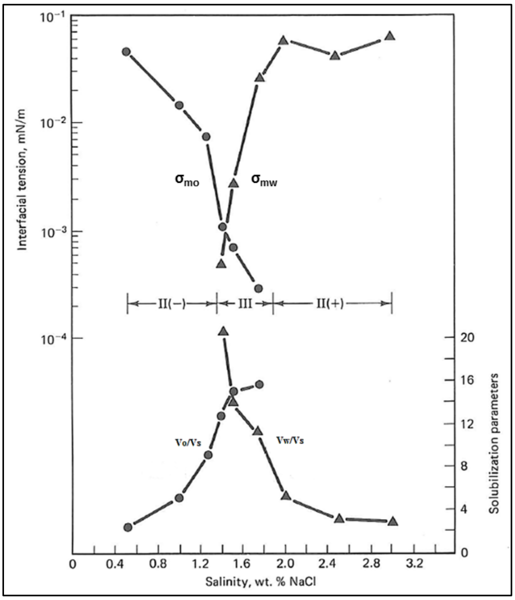

Figure 3.2 – The relation between IFT, solubilization parameters and phase behavior. Taken from Reed and Healy [32].

The solubilization parameter, SP_i, express the volume of oil or water solubilized in the microemulsion per unit volume of surfactant, and is given by

$$SP_i = \frac{V_i}{V_s} \tag{3.2}$$

where *i* refers to oil or water, and *s* refers to the surfactant. The point in Figure 3.2 where $SP_o = SP_w = SP^*$, i.e. where the microemulsion contains equal amounts of oil and water (Winsor III), is also represented by a minimum in IFT and is referred to as optimal salinity [19]. SP^* is the solubilization parameter at optimal salinity.

As mentioned above Huh [31] introduced an empirical relationship between SP^* and σ

$$\sigma = \frac{C}{(SP^*)^2} \tag{3.3}$$

where C is an empirical constant, usually 0.3 mN/m. This relationship serves as useful a tool for calculating IFT at optimal salinity based parameters obtained from the phase behavior experiments. However, IFTs other than at optimal salinity, for instance in a low salinity environment or for low concentration microemulsion systems where the three-phase area is too small to be visually detected, IFT measurements must still be conducted. Vice versa IFT measurements can be employed to find the optimal salinity by a minimum in a graph displaying IFT as a function of salinity [23].

Traditionally, the Winsor III region has been the target when tailoring a surfactant system to optimize oil recovery by surfactant flooding due to ultralow IFT and excellent microemulsion phase behavior with crude oils [6,23,33,34]. However, ultralow IFT occur at a narrow range of salinities [5], and many surfactants in this region are not sufficiently soluble at optimum salinity to give clear stable aqueous solutions [35]. Another problem that affects the efficiency of surfactant flooding is the loss of surfactant by retention mechanisms like adsorption, phase trapping, precipitation, thermal degradation and dispersion of surfactant where many of these mechanisms increase with increasing salinity [33,36,37].

A surfactant flood in a Winsor I environment is the simplest type and is straightforward because the surfactant is transported and remains in the aqueous phase [5] and the systems conditions exists throughout the flood. Also, the retention is much lower in these floods. The drawback of this design has been that the moderate reduction in IFT in these systems are usually not low enough for good oil displacement [37].

4. THE LOW SALINITY EFFECT (LSE)

Waterflooding of oil reservoirs by seawater (SW) is the most frequently applied recovery method for improved oil recovery. Traditionally, little attention has been given to the composition of the injection water and its possible effects, until Morrow and his co-workers [38-42] observed from experiments that oil recovery depended on water composition. Following this, the possible benefit of waterflooding with LS brine has drawn the oil industry and researches attention initiating studies [43-49] with objectives to confirm the benefits and find the mechanisms of such benefits [50].

4.1 Proposed mechanisms for the LSE

Complex crude oil/brine/rock (COBR) interactions and conflicting observations from experimental studies complicate the understanding of the LSE. There is no clear consensus about the dominant mechanisms and the LSE likely results from a combination of more than one mechanism [49]. Still, many of the results indicate that certain conditions are needed to get a positive response on the oil recovery by using LS water injection. The conditions cannot guarantee the LSE, and in some cases, all of them are not necessary. They include [51]:

- Non-zero initial water saturation.
- The salinity of the injection water must be lower than that of the connate water, and with a certain ratio.
- Crude oil, containing naturally occurring surface-active agents, acids and bases to create mixed-wet conditions.
- Clastic materials, containing active clay materials and Kaolinite in particular.

The main suggestions explaining the underlying mechanisms for the LSE include the double layer expansion, multicomponent ionic exchange (MIE), fines migration, effect of pH variation and wettability alteration.

4.1.1 DLVO and the double layer expansion

Several experimental studies on the LSE in recent years have concentrated on the mechanisms which change the stability of thin brine films that wet the surface of the reservoir rock, and, in particular, the double layer expansion [47,49,52-54].

Double layer expansion is described by classical DLVO (Derjaguin-Landau-Verwey-Overbeek) theory which concerns colloidal stability and explains interactions between colloidal particles, their aggregation behavior and the forces between charged interfaces interacting through a liquid medium. It combines the effects of the van der Waals attraction and the electrostatic repulsion due to the double layer of counter ions.

The way double layer expansion can explain the LSE is by the counter ions in the brine film that adsorb to the negatively charged brine/oil and brine/rock interfaces and screen the repulsion between these two negatively charged interfaces. A characteristic length of this screening is called the diffuse or electrical double layer. Figure 4.1 shows the electrical potential of a negatively charged surface versus the distance from the charged surface. Double layer thickness is thus related to the electrical charges at the interfaces which can be estimated measuring the zeta potential. This is the potential at the shear plane of the electrical double layer [47].

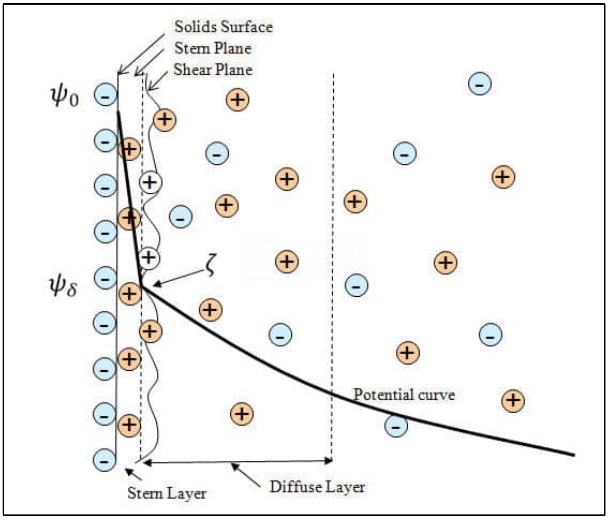

Figure 4.1 – Electrical double layer according to Stern's model [55].

When the brine salinity is lowered, the diffuse double layer increases since the ionic strength in the solution decreases. Both double layers expand to become more diffuse. As a result, the two interfaces experience greater electrostatic repulsion. Consequently, the water film becomes thicker and more stable, resulting in a more water-wet rock [49], thus leading to a destabilization and mobilization of the oil adhered to the rock.

4.1.2 Multicomponent Ion Exchange (MIE)

Another proposed mechanism to explain the LSE involves the non-DLVO interactions between the brine/oil and brine/rock interfaces, namely Multicomponent Ion Exchange (MIE), which has together with the double layer expansion been referred to as thin-brine-film mechanisms [49]. Lager et al. [56] proposed MIE as the predominant mechanism underlying the improved waterflood recovery observed by injecting LS water.

Crude oil forms organometallic complexes with divalent cations, such as Ca^{2+} and Mg^{2+}, that are adsorbed on the clay surface promoting oil-wetness on rock surfaces [50,56]. Other organic polar components in the oil are adsorbed directly to the mineral surface without cations being present causing an even more oil-wetness of the clay surface. During LS injection MIE takes place, replacing complexed cations/bonding with un-complexed cations from the injection water. The surface becomes more water-wet by desorption of the organometallic complexes, resulting mobilization of the oil adhered to the rock.

4.1.3 Fines mobilization and migration

Clay tends to hydrate and swell when contacting fresh water. If the ionic strength of the injected brine is less than the critical flocculation concentration the clay can become destabilized and migration of clay can occur. The critical flocculation concentration is strongly dependent on the relative concentration of divalent cations. Divalent cations lower the repulsive force by lowering the Zeta potential. Therefore, they have been known to stabilize clay [50,57].

The hypothesis of fines migration as a mechanism for LS injection is meant to explain an increase in oil recovery by either wettability alteration and/or diversion of flow.

The wettability state of the system is assumed to reside in the weakly water-wet regime. Within this wettability range, mixed-wet particles are formed by adsorption of heavy polar components from crude oil on the rock surface that is not overlain by bulk connate water. Upon injection of low salinity brine, the electrical double layer in the aqueous phase between particles will expand and the tendency for stripping of fines is increased. This will lead to wettability change towards more water-wet condition. Detachments of these particles from the pore walls will then contribute to increased oil recovery [42], see Figure 4.2.

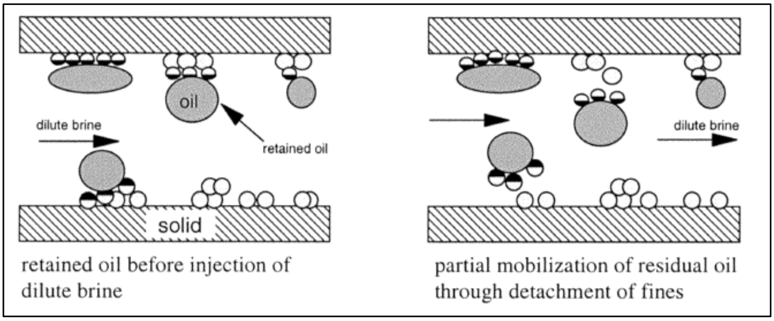

retained oil before injection of dilute brine

partial mobilization of residual oil through detachment of fines

Figure 4.2 – Role of mobile fines in COBR interactions and increase in oil recovery with decrease in salinity. Taken from [42].

Accumulation of the fine particles in pore constrictions is thought to result in diversion of flow, which may direct the flowing fluid to new areas of flowing channels. As a result, an increase in oil production is registered. This may after all not be a favourable effect since it is accompanied with a reduction in formation permeability due to clay dispersing the in water can lodge smaller pores and pore throats. Reduction of permeability and produced fines were observed in this work during a water sensitivity study, see chapter 6.2.1.

4.1.4 Variation in pH

Based on the work of Austad et al. [48,58], Myint et al. [49] named the following mechanism the Austad et al. mechanism. It proposes a chemical mechanism where the clay acts as a cation exchanger and produces a local increase in pH close to the brine/clay interface.

When the salinity decreases by LS injection, the equilibrium between the adsorbed polar components in the oil and inorganic cations in the formation brine (Ca^{2+}) is disturbed because the concentration of cations in the brine is lowered. To counteract this disturbance, there is a net desorption of cations, especially Ca^{2+}. To compensate for the loss of cations, protons, H^+, from the water close to the clay surface adsorb onto the negative sites of clay, causing a local increase in the pH. The local increase in pH induces acid/base reactions that result in the release of basic (Figure 4.3 - upper) and acidic (Figure 4.3 - lower) groups in oil from the clay surface. The net result is oil release and wettability alteration due to breakage of non-DLVO interactions (acid/base interactions, hydrogen bonds) between the brine/oil and brine/clay interfaces. The mechanism is illustrated in Figure 4.3.

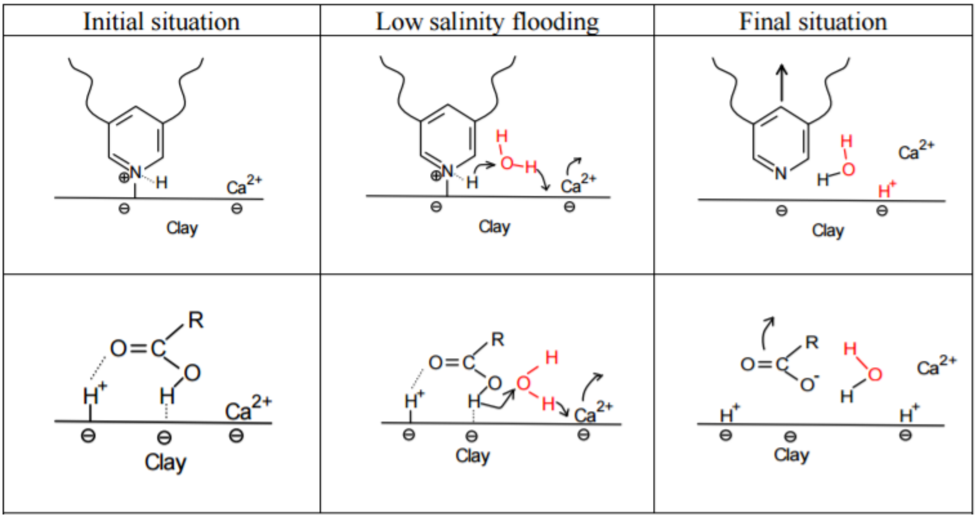

Figure 4.3 – Proposed mechanism of local variation in pH. Upper: Desorption of basic material. Lower: Desoprtion of acidic material. Taken from [58].

In addition, the Austad et al. mechanism alters the brine/clay electrostatic potential because substitution of an adsorbed divalent cation with H^+ makes the clay surface even more negatively charged. This enhances the double-layer expansion [49].

In some reported studies LS injection is accompanied by rise in pH [42,44], but the change in pH cannot be used to explain the LSE alone [59,60].

4.1.5 Wettability alteration

Wettability alteration towards increasing water-wet state during LS injection is the most frequently suggested cause of increased recovery. When wettability changes from less to more water-wet conditions, oil is released from rock surfaces and recovery is increased. Evidence for wettability change is, however, often indirect such as from changes in relative permeability curves or centrifuge capillary pressures [51]. All of the proposed mechanisms above explain the wettability alteration as a result of the mechanism(s) and not the mechanism itself, so wettability alteration is the effect rather than the cause.

5. MATERIALS AND METHODS

This chapter will explain the main materials and chemicals used in this work together with experimental setup and how experimental methods have been performed.

5.1 Salt Water

The seawater (SW) used in this work is made up of Na^+, Ca^{2+}, Mg^{2+}, K^+, Cl^-, SO_4^{2-} and HCO_3^- ions, to a total of around 36 000 ppm which.

The low salinity (LS) water used in the initial core flooding experiments was around 3000 ppm NaCl. Due to the possibility that divalent ions eluted from the core material could interfere with the interfacial properties of the surfactant system [61,62], it was decided to use diluted SW as LS water further, i.e. LS water containing divalent ions. The ionic strength of the two versions of LS water was still more or less the same, i.e. around 0.05 mol/kg, resulting in LS water of around 2500 ppm diluted SW. Equation (5.1) shows the equation used for calculating the solution ionic strength, *I*:

$$I = \frac{1}{2}\sum_{i=1}^{n} c_i\, z_i^2 \tag{5.1}$$

where *c* is the molality and *z* is the charge of element *i*.

The injection waters other than SW and LS water mentioned above, were also dilutions of SW of different degrees depending on phase behavior, see Table 5.1.

5.2 Surfactant Phase Behavior

All surfactant phase behavior test samples were prepared in specially designed, graduated tubes. For the main surfactant phase behavior tests the aqueous surfactant solutions were mixed with an equal volume of crude oil and stored in heating cabinets at the appropriate temperatures for the core flooding experiments. Solubilization parameters (SP_i) were obtained by measuring the phase heights in the samples after equilibration was reached. For the surfactant systems where it was possible, optimal salinity (S^*) was determined by the intersection point between SP_w and SP_o when plotted as a function of salinity.

The compositions of surfactant solutions, oil phases and IFT between them for the different core flooding experiments are shown in Table 5.1.

Table 5.1 - Surfactant solution composition, oil phase and IFT between them, for the surfactant solutions used in the core flooding experiments in this thesis

Surfactant composition	**Surf. conc. [wt%]**	**Co-solvent**	**Salinity [ppm]**	**Oil phase**	**IFT [mN/m]**	**Core ID**
Paper 1						
S13	0.2	-	3 000 NaCl	STO A	0.015	A1
S13	1	-	3 000 NaCl	STO A	$5 \cdot 10^{-4}$	A1
Paper 2						
3:1 APS:IOS	0.2	SBA	2 500 sw	STO A	0.018	L1, L3, H1
3:1 APS:IOS	0.2	SBA	15 500 sw	STO A	$3 \cdot 10^{-4}$	L2, H2
Paper 3						
3:1 APS:IOS	0.5	SBA	2 500 sw	STO B	0.12	LS1
APS	0.5	IAA	2 500 sw	STO B	0.025	LS2
2:5 APS:IOS	0.5	SBA	25 800 sw	STO A	0.06	HS1
1:1 APS:IOS	0.5	IAA	15 300 sw	STO B	0.015	HS2

The surfactant in paper 1 was a propoxylated isotridecyl alcohol sulphate surfactant with 13 propoxy (PO) groups (S13).

The surfactant blends in paper 2 and 3 all consisted of different ratios of alcohol propoxy sulfate (APS) with a C_{12-13} hydrocarbon chain with 7 propoxy (PO) groups, and internal olefin sulfonate with a C_{15-18} hydrocarbon chain (IOS).

5.3 Interfacial Tension (IFT)

A spinning drop tensiometer (SITE100 from KRÜSS) was used to measure IFT between the surfactant solution and the oil. The IFT calculations are based on the Young-Laplace equation which is given by

$$\Delta p = \sigma \left(\frac{1}{R_1} + \frac{1}{R_2} \right) \tag{5.2}$$

where Δp is the pressure difference across the fluid interface, σ is the interfacial tension between the two phases and R_1 and R_2 are the radii of curvature.

Each sample was allowed to spin until the phases had reached equilibrium, usually taking around one hour. The values measured here were used to calculate the different capillary numbers and thus the CDC plots. IFT values were also used to determine phase behavior systems at low surfactant concentrations, see Figure 6.4.

5.4 Core Preparations

After weighing and measuring dimensions of a dry core sample, it was mounted in Hassler core holders with an overburden pressure of around 25 bars, vacuumed and saturated with SW to determine the porosity. After at least one week of rock/brine equilibration time, absolute permeability at 100% water saturation, K_w, was measured before the core was drained with oil to establish initial water saturation S_{wi}.

It is generally accepted that a wetting condition other than strongly water-wet is a requirement for the core material in order for the LSE to occur [63]. All cores in this work were therefore subjected to elevated temperature obtaining wettability states other than strongly water-wet. The procedure included aging time for at least two weeks in 110^{0}C (except core A2, see chapter 6.3.1) with flushing of fresh oil through the core both during and after the aging process.

Core flooding experiments were carried out at an injection rate of 0.1 ml/min while continuously measuring dP over the core and conducting relative permeability measurements after each injection step. Low Salinity Surfactant flooding experiments, referred to as LSS injection, in tertiary mode involves an initial SW flood, followed by a waterflood at reduced salinity, and finally surfactant injection at reduced salinity. For similar experiments in secondary mode the SW flooding step is omitted.

Surfactant flooding in a salinity environment too high for the LSE to be expected is referred to either HSS or OSS depending on the phase behavior, Winsor I (HSS) or Winsor III (OSS). Thus, these experiments represent closer to classical surfactant injection experiments.

5.5 Wettability

To get an indication of the wetting state of the core material using the aging method described above, a wettability test based on spontaneous imbibition measurement was conducted, see chapter 6.2.2. A wettability study obtaining the full set of capillary pressure curves was not performed; however, it was decided to do spontaneous imbibition tests on one aged and one non-aged Berea core plug cut from the same block, to obtain a wettability *indication* after the aging process. The steps included in this test were primary drainage, spontaneously imbibition and forced water injection. After primary drainage, one of the core plugs was not subjected to elevated temperature and was therefore assumed to be strongly water-wet [64]. The other core plug was aged at 110 ˚C for two weeks, similar to the rest of the cores in this work.

Oil recovery by spontaneous imbibition, followed by a waterflood was studied here to obtain the Amott wettability index to water, I_w, for the two cores:

$$I_w = \frac{\Delta S_{ws}}{\Delta S_{ws} + \Delta S_{wf}} \tag{5.3}$$

where the subscript *s* and *f* refers to whether the change in fluid saturation is a spontaneously or forced process.

If nearly all of the oil recovered occurs by spontaneous imbibition, I_w is close to 1.0 and the system is described as very strongly water-wet [65]. Systems are increasingly less water-wet as I_w approaches 0. Similarly, an Amott oil wettability index, I_o, can be defined by measuring spontaneous imbibition of oil, followed by forced displacement of water by oil. If both indexes are obtained the Amott-Harvey wettability index can be calculated by

$$I_{AH} = I_w - I_o \tag{5.4}$$

5.6 In-Situ Saturation Monitoring

Three cores in P3 were subjected to in-situ saturation monitoring. The in-situ fluid saturations were determined using an X-ray scanning technique and a semi-log interpolation method based on Labert's law.

The detector system was mounted on a trolley, which moved by a step motor along the sample. Intensities were measured every 0.5 cm. When starting a scan, X-rays are emitted from a 70 kV, 0.1 mA MiniFocus Tungsten target source. A detector measures the intensities of the X-rays passing through the sample. After the predefined count interval of 3 s, the X-ray device moves to the next position.

The material the X-rays pass through from source to detector attenuates them. The reduction in intensity of an X-ray beam as it passes through a core depends upon the fluids present. To improve the accuracy of the saturation determination in this study, the oil phase was doped with iododecane, which enhances the attenuation contrast between oil and water. To compute the oil saturation during a flooding process, reference scans of the dry core, 100% saturated with brine and at S_{wi} were required. The uncertainty in the saturations can therefore be calculated from the scans as well as from the material balance in these experiments. The oil saturation at S_{wi} at each measured point is given by distributing the average oil saturation from the material balance according to the difference in counts between the 100% water-saturated scans and the scans at S_{wi}, see Equation (5.5).

$$S_{o,S_{wi}} = \bar{S}_{o,S_{wi}} - \frac{ln\frac{\bar{I}_{100\%\,water}}{\bar{I}_{S_{wi}}} - ln\frac{I_{100\%\,water}}{I_{S_{wi}}}}{\frac{\bar{I}_{100\%\,water}}{\bar{I}_{S_{wi}}}} \tag{5.5}$$

I is the intensity counted by the detector and the subscripts denote the saturation state of the core. At each measured point during the flooding experiment the oil saturation is given by, (5.6).

$$S_o = S_{o,S_{wi}} \frac{lnI - lnI_{100\%\,water}}{lnI_{S_{wi}} - lnI_{100\%\,water}} \tag{5.6}$$

5.7 Water Sensitivity

A water sensitivity study was conducted on a 600 mD Berea core plug to investigate the C_{sc} representative for the core plugs and brine used in this work, see chapter 6.2.1. The core was 100% saturated with SW and flooded with SW brine the first PVs. Then, the injection brine was changed to 1 wt% NaCl and thereafter gradually changed to decreasing NaCl concentrations ending with distilled water free from salt. The dP over the core was continuously measured during the injection period to calculate the permeability.

5.8 Retention

Dynamic retention experiments were performed in two Berea cores, R1 and R2, both holding absolute permeabilities around 100 mD. R1 and R2 were saturated with LS and OS brine, respectively. Retention profiles, Figure 6.11, were obtained by injecting a surfactant slug (R1 = 5 PV and R2 = 6 PV) into the core which had a salinity corresponding to the surfactant solution salinity. The slugs contained the same components and concentrations as in the flooding experiments and were followed by a continuous injection of chase water with the appropriate salinity. The effluent was collected in fractions to be analysed for total surfactant content by potentiometric titration.

5.9 Dispersion

To gain better understanding of the fluid flow in the core material, dispersion measurements were conducted by measuring the effluent resistance when brine with a different salinity than the connate brine was injected. The measurements were conducted both at S_{or} and at 100% water saturation to investigate the effect of residual oil on fluid flow.

Dispersion curves are obtained by plotting the measured resistance as a function of PV, and are analysed based on break-through and shape. In a homogeneous core displaying ideal dispersion, half of the injected concentration breaks through after 1 PV with the profile being symmetrical around this point [66]. Earlier break-through is associated with the presence of isolated pores that are not participating in flow, meaning that the effective PV during flow is less than the total PV. Tailing of the tracer profile, i.e. deviation from symmetry, is due to mass exchange with dead-end pores, which can be due to for example the presence of laminations.

6. SUMMARY OF MAIN RESULTS

The main aim of this thesis was to investigate whether LS flooding in the presence of surfactant could be an attractive EOR technique compared to low salinity or surfactant flooding applied alone. The hypothesis is that;

- Oil layers destabilized by LS flooding can be trapped before they are produced. Lowering the IFT in this process would reduce the trapping
- Traditional surfactant flooding at ultralow IFT yields very high recoveries, however it is usually associated with high cost
- Surfactant systems in LS environments are easier to control at lower costs than traditional surfactant systems. The drawback is that the moderate reduction in IFT in these systems are usually not low enough for good oil displacement
- Combining the techniques of LS and surfactant flooding takes advantage of the destabilized oil by LS injection and with only a moderate reduction in IFT by surfactant flooding can mobilize the destabilized oil and/or reduce the trapping of mobilized oil.

The results obtained throughout this work are presented in three scientific papers: All papers start with surfactant phase behavior and core characterization studies which are summarized in chapter 6.1 and 6.2 respectively. Following this, the results from the core flooding experiments where the combined effect of LS flooding and reduced capillarity on oil production are discussed.

In the first paper (P1), we showed that LS injection alone did not contribute to additional oil recovery in tertiary mode, however, LSS injection gave an increase in oil recovery beyond what was expected based on lowering the IFT alone. These results suggest a combined effect of LS and surfactant injection which exceed oil recoveries of either of the techniques applied alone. Mixed-wet conditions appear to be more favorable than water-wet conditions for the combined process to occur.

The observations were taken further in the next paper (P2) where we compared oil recovery at LS conditions with moderate IFT reductions (Winsor I surfactant system), to oil recovery at high salinities and ultralow IFT reductions (Winsor III surfactant system). The results showed comparable recoveries for LSS flooding at capillary numbers 2 orders of magnitude lower than that for surfactant flooding at ultralow IFT, and we could conclude that the LSS process appears more efficient than a traditional surfactant flooding process.

In the final paper (P3) we compared the combined effect of reduction in IFT and LS injection, to the effect of a sole reduction in IFT. The reductions in residual oil saturations, at similar capillary numbers and phase behavior conditions, are higher for the LSS experiments compared to regular injection experiments. Based on these results we concluded that the two strategies follow different CDC´s with the LSS experiments giving rise to lower residual oil saturations than the HSS experiments.

6.1 Finding Suitable Surfactant Systems through Phase Behavior Studies

The properties of a surfactant system are often sensitive to changes in its chemical composition. Thus, thorough preparations of surfactant phase behavior tests are a prerequisite before conducting dynamic flooding experiments involving surfactant systems. Static surfactant phase behavior tests were performed for all surfactant formulations used in this thesis.

Since the aim of the core flooding studies was to investigate the combined effect of LS brine and surfactant, the main objective for most of the surfactant phase behavior studies was to find a surfactant solution that would, at LS conditions, reduce the water-oil IFT to a moderate level and form a lower phase microemulsion (Winsor I) with the crude oil in question. To investigate the effect of a moderate water-oil IFT combined with LS brine, it was important to avoid the three phase microemulsion area (Winsor III) where ultralow IFT values $< 10^{-2}$ mN/m occur, which normally is the target in traditional surfactant flooding processes. At the same time the classical requirements for phase behavior tests applied; stable aqueous surfactant solutions with no precipitation or phase separation at the given temperature and salinity with an equilibration time as short as possible [35]. Also, as few components in the surfactant solution as possible are preferred to increase the systems robustness with regards to chromatographic separation [36]. Few components are also preferred in a more practical aspect to get a simpler and manageable logistics for off-shore operations.

6.1.1 Low Salinity Winsor I Phase Behavior System (P1)

The main objective of the core flooding experiments in P1 was to investigate the combined effect of LS injection and reduced capillarity, and to investigate to which extent the capillary forces needs to be reduced to take advantage of the increased recovery by combining the two methods. Phase behavior studies were therefore conducted to find a Winsor I surfactant system showing a gradual decrease in IFT while staying in the LS region.

IFT measurements using the S13 surfactant (isotridecyl alchol 13PO sulphate) at a constant LS salinity of 3000 ppm NaCl and crude oil STO A, showed a decreasing IFT with increasing surfactant concentration from 0.2 to 1 wt%, see Figure 6.1. The phase behavior samples at these conditions were all in the Winsor I regime characterized by transparent water phases with a yellow colour due to solubilized oil, and no indications of viscous phases. This was achieved without the use of co-solvents or co-surfactants. Thus, the surfactant system fulfilled the requirements for this study and was selected for the LSS core flooding experiments.

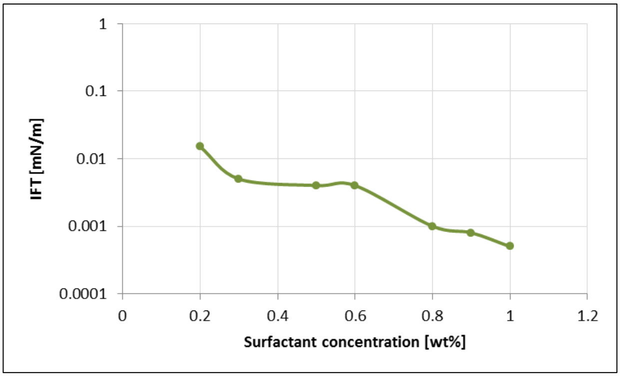

Figure 6.1 – IFT values between S13 surfactant solution at 3000 ppm NaCl and crude oil (STO A), as a function of surfactant concentration.

Changing one component in a surfactant system, like the surfactant concentration in this case, may cause a change in the phase behavior of the system. The change in IFT in Figure 6.1 may be an indication of that. Even though the IFT gradually changes, a phase transition from Winsor I to Winsor III [32] was not observed in the phase behavior sample tubes. However, the transition zone between Winsor I and III may nevertheless move towards lower salinities with increasing surfactant concentration.

In pure surfactant, water and hydrocarbon systems, IFTs decreases monotonically with surfactant concentration up to the formation of surfactant micelles, i.e critical micelle concentration (CMC). Interfacial properties of natural petroleum sulfonate systems are generally similar to those of pure surfactant systems. However, because of the multicomponent nature of petroleum sulfonate systems, a sharp CMC may not be observed, and IFT may change with surfactant concentration even well above the CMC region [21,32].

6.1.2 Winsor I and Winsor III Phase Behavior Systems (P2)

The objective of the core flooding experiments in P2 was to compare the efficiency of the low salinity surfactant (LSS) injection process, with the more traditional surfactant injection approach at optimal salinity (OSS), in terms of increased oil recovery and surfactant retention.

To achieve this, a surfactant formulation which could simultaneously show low IFT and Winsor I phase behavior in the LS region, and Winsor III phase behavior with ultralow IFT at salinities outside the salinity range normally associated with a LSE, had to be used. Due to unfavourable phase behavior outside the Winsor I region using the S13 surfactant (P1), a new screening process was initiated resulting in using a mixed surfactant formulation of APS (Alcohol Propoxy Sulphate) and IOS (Internal Olefin Sulfonate) that were fit for this purpose.

Effect of surfactant concentration and WOR on phase behavior

High surfactant concentrations (2-5 wt%) and WOR of 1:1 are often standard conditions in initial surfactant screening processes. These are not necessarily realistic conditions in further experiments, but is used to obtain clear visual phase behavior characteristics, and to keep consistency throughout a screening process [67,68].

The target surfactant concentration for the core flooding experiments in P2 was 0.2 wt%. To investigate the effect of reducing the surfactant concentration, a phase behavior study using surfactant concentration as the variable parameter was conducted. It was reduced from 3.3 wt% to 0.2 wt% which promoted a shift in phase behaviour from Winsor I –> III –> II, and the optimal salinity (S^*) came close to the LS region for the target surfactant concentration, see Figure 6.2. This was an undesirable situation due to the objective of a Winsor I regime in the LS region and a Winsor III regime well outside the LS region. Here the WOR was constant at 1:1.

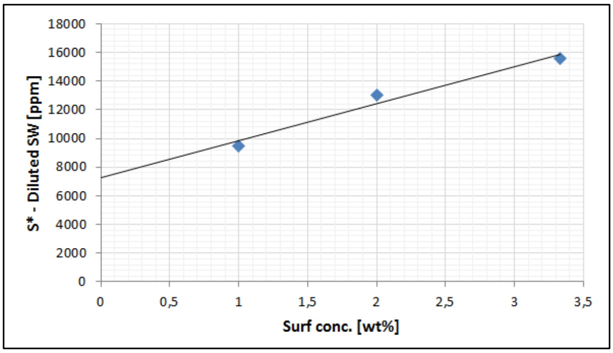

Figure 6.2 - Optimal salinity as a function of surfactant concentration. The extrapolated line indicates the optimal salinity with decreasing surfactant concentration at a WOR = 1.

Testing the WOR as the variable parameter however, the opposite behavior was observed. Increasing the WOR, which is a more realistic condition when flooding at $S_{orw,}$ a phase behavior shift of Winsor II –> III –> I was observed, see Figure 6.3. Here the total surfactant concentration was held constant at 3.3 wt%.

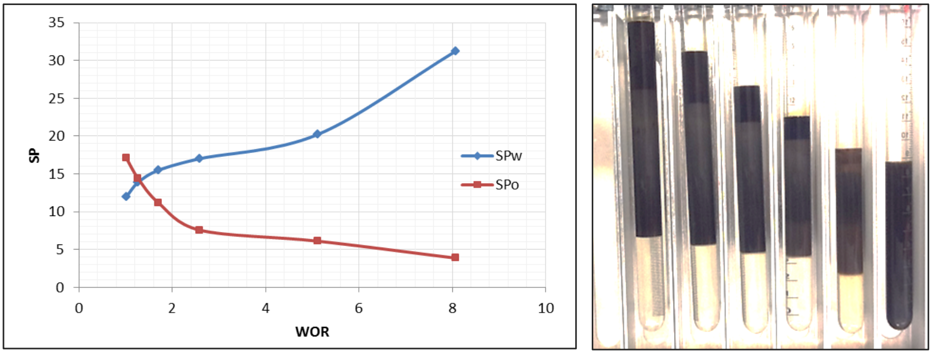

Figure 6.3 – SP for water and oil at increasing WOR (left). Phase behavior tubes with increasing WOR (right).

Varying the two parameters promoted opposite shifts in the phase behavior. IFT measurements were conducted to conclude on the phase behavior for this system.

IFT as a function of phase behavior

Phase behavior can also be investigated in terms of measuring the IFT between the surfactant solution and the oil at increasing salinities [21]. In this work these measurements concluded on the moderate and ultralow regions for the given surfactant system.

The IFT is also an essential term when the capillary number, N_c, i.e. the efficiency of a surfactant flood is evaluated.

The IFT measurements for the surfactant blend discussed above are shown in Figure 6.4 as a function of salinity. The IFT at LS salinity (around 2500 ppm diluted sw) was measured to 0.018 mN/m. A minimum in IFT was found at a salinity around 15 600 ppm diluted sw, i.e. optimal salinity (OS), with a value in the ultralow region (IFT = 3×10^{-4} mN/m)**.** The salinity corresponding to a minimum in IFT is referred to as the optimal salinity (OS), and is also the salinity where the middle phase microemulsion was found in the high surfactant concentration phase behavior tests.

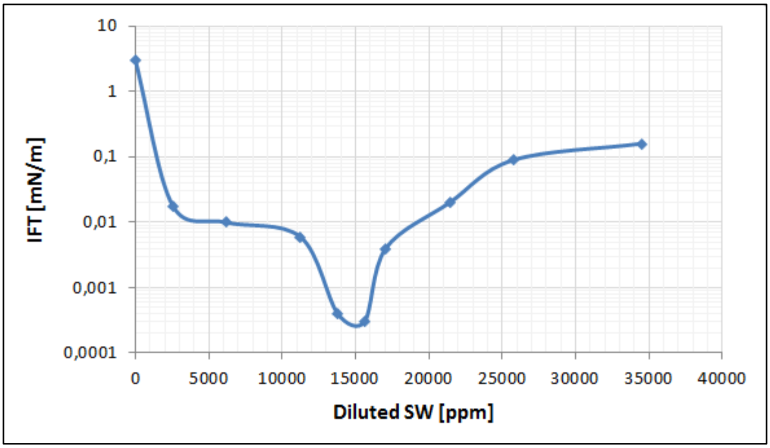

Figure 6.4 – IFT as a function of salinity for the 0.2 wt% APS 7PO blend and crude model oil.

Based on the phase behavior studies and IFT measurements, the surfactant system including APS (7 PO groups), IOS and SBA showed suitable behavior for this study’s purpose and was selected for the core flooding experiments. It showed a moderately low IFT in the LS region and an ultralow IFT in the OS region. In addition, there was a good distance in terms of salinity between the OS and LS region to make sure that there is no effect of reduced salinity on oil recovery in the OS case.

6.1.3 Low- and High Salinity Winsor I Phase Behavior Systems (P3)

In P3, X-ray scans were performed during the core flooding experiments to investigate in-situ changes in the oil saturation pattern. To improve the contrast in the x-ray signals between crude oil and water, iododecane had to be added to the crude oil. Consequently, the crude oil, STO B, had to be used in phase behavior studies.

Also, the objectives of P3 was to compare LSS core flooding experiments with surfactant flooding experiments at a salinity higher than the LS salinity, while still being in the Winsor I regime (HSS). New conditions and objectives lead to new rounds of phase behavior studies.

The combination of APS and IOS surfactants showed promising behavior and recovery results in P2 [28] in this thesis, as well as in other studies [6,68-70]. Different ratios of APS and IOS were therefore used to tailor the surfactant systems to moderate IFTs to Winsor I systems in the salinity range mentioned above. The surfactant phase behavior results for the surfactant systems used in the core flooding experiment are found in Table 6.1, while the flooding salinity and IFT used in each of the cores are found in Table 6.2.

Table 6.1 – Phase behavior results for different APS:IOS ratios, co-solvents and oil compositions. A 1:1 surfactant to co-solvent ratio, and a total surfactant concentration of 3.3 wt% was maintained in all experiments

Surfactant system APS:IOS ratio	Co-solvent	Oil phase Crude	S*, Diluted sw [ppm]	SP*
2:5	SBA	STO A	54 000	11
3:1	SBA	STO B	27 475	13
1:1	IAA	STO B	17 205	10.5
1:0	IAA	STO B	7 347	●

- SP* was not calculated due to a narrow salinity window. Only one tube displayed three phases for this system which is at the salinity listed in the table.

Table 6.2 shows the flooding conditions for the four cores, LS1, LS2, HS1 and HS2. The LS cores represent flooding conditions using LS brine (approx. 2500 ppm SW), while the HS cores represent flooding conditions outside the LS region, but still in the Winsor I regime at moderate IFT's.

Table 6.2 – Surfactant system, flooding salinity and IFT against the crude oil at this salinity for each ore flooding experiment

Surfactant system APS:IOS ratio	Flooding salinity (ppm)	IFT (mN/m)	Core ID
3:1	2549	0.12	LS1
1:0	2549	0.025	LS2
2:5	25866	0.06	HS1
1:1	15302	0.015	HS2

6.2 Improved Understanding of Core Flooding Experiments through Core Characterization and Effluent Analysis

In this chapter, some of the results from methods conducted to analyse the core material and effluent water after flooding experiments are presented. A water sensitivity experiment was performed to investigate the salinity's effect on the core material. To get an indication of the wettability alteration in the core material using the aging method described earlier, a wettability test was performed on two cores where only one followed the aging method described above. To calculate the retention of surfactant during a flooding experiment, surfactant concentration in effluent water was measured after all core flooding experiments. Dispersion measurements were conducted after the core flooding experiments to investigate heterogeneities in the core material.

6.2.1 Water Sensitivity

Water sensitivity of sandstones is a colloidal phenomenon where the permeability of the sandstone decreases at a specific salt concentration, termed Critical Salt Concentration, C_{sc} [71]. This is an important phenomenon in LS studies, because the concentration of brine used in LS experiments may be close to the C_{sc} of the core material.

Figure 6.5 shows the result of a water sensitivity experiment on a Berea sandstone core with permeability as a function of injected volume of decreasing brine salinity. The core is initially saturated with SW, $S_w = 1$. Permeability reduction was first observed during the 0.3 wt% NaCl injection, which is the LS brine concentration used in this study. Additional brine salinity reduction lead to additional reduction in permeability, however, fines were only visually observed in the distilled water effluent, see photograph in Figure 6.5. An Energy Dispersive Spectroscopy (EDS) analysis confirmed that the deposit in the effluent water was Kaolinite.

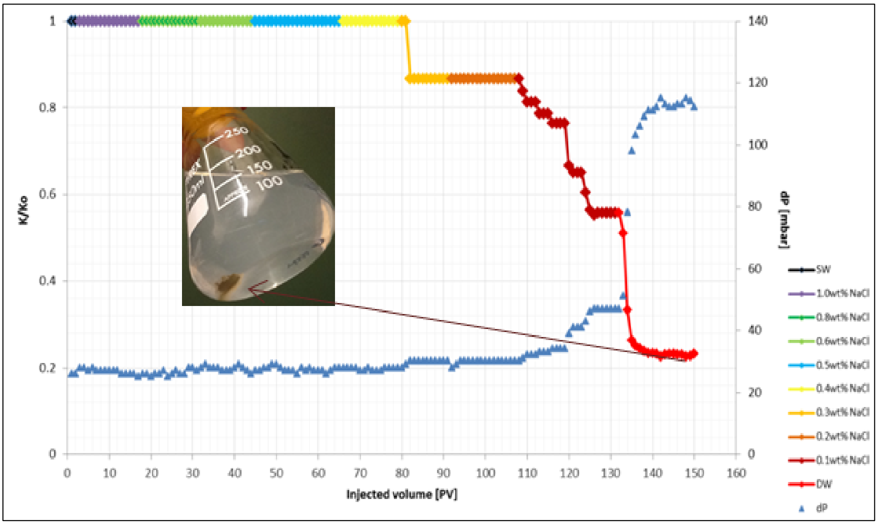

Figure 6.5 – Permeability reduction and differential pressure as a function of injected volume of decreasing salinity.

The increases in dP, i.e. permeability reduction, is mainly attributed to the release and mobilization of clay particles, mainly Kaolinite, that occurs when the salt concentration falls below the C_{sc} [57,71,72]. The C_{sc} is strongly dependent on the relative concentration of divalent cations such as Ca^{2+} and Mg^{2+} [73]. The mechanism of fines mobilization and migration is explained by the DLVO theory of colloids, which was mentioned in chapter 4.1.1. The counter ions (e.g. Ca^{2+} and Mg^{2+}) involved in the interactions between solid and aqueous phase contribute to low repulsive forces in the double layer. When the brine salinity is lowered, the double layer will expand, and the tendency for release of fines is increased. This test indicates that there are brine/rock reactions taking place inside the core material that are explained by mechanisms that are also suggested for the LSE when reducing the injection salinity enough. It also shows a low degree of core material damage during injection of 0.3 wt% NaCl brine.

6.2.2 Wettability

It was important with an indication of the wettability obtained from the aging procedure described in chapter 5.4 since the hypothesis of the LSE in this work is that oil layers adhered to the rock surface are destabilized in the presence of LS water. This implies that oil initially is adhered to the mineral surface of the core, i.e. the core is not strongly water-wet.

There are no direct measurements of wettability in cores [74], however the Amott [75] and USBM test [76] are methods of characterizing wettability of crude-oil/brine/rock (COBR) systems. Both depend on capillary pressures and microscopic displacement efficiencies where the full sets of capillary pressure curves are obtained.

Morrow et al. [65] proposed a test were only the Amott wettability index to water, I_w, together with the imbibition rate is used to characterize the wettability of a core. Others [39,63,65,74] have adopted this test to characterize the wettability of core plugs. The objective of the test in this work was to compare the wettability, I_w, in a core (w1) after subjected to the aging procedure described in chapter 5.4, to a core not subjected to this aging procedure (w2).

The wettability of a porous medium will affect its waterflood behavior and relative permeability because it is a major factor in the control of the location, flow and distribution of fluids. In a uniformly wetted core, the effective oil permeability at a given initial water saturation decreases as the wettability is varied from water-wet to oil-wet [77]. Measurement of oil relative permeability, k_o, before and after aging can therefore give an indication whether the wettability has been altered during the aging process. S_{wi} is assumed unchanged during this process in such a way that a direct comparison of k_o before and after aging can be made. Table 6.3 shows the permeabilities measured for w1 and w2. A reduction in k_o of around 50% after aging is measured for w1, and is typically observed for the other cores in this thesis as well.

Table 6.3 – Experimental data for calculating Iw for w1 and w2

Core ID	Aging time [days]	$k_{o\ (Swi)\ before\ aging}$	$k_{o\ (Swi)\ after\ aging}$	I_w
w1	14	165	90	0.42
w2	0	120	not aged	1

Figure 6.6 shows the oil recovery, as a function of spontaneous imbibition time for core w1 and w2. For systems that spontaneously imbibe, rate of imbibition provides a useful measure of degree of wetting [78]. The imbibition rate and oil recovery by spontaneous imbibition are higher for the non-aged core, i.e. the water-wet core. The induction time is also longer for the aged core. These results are consistent with earlier published data for Berea sandstone cores [41,65].

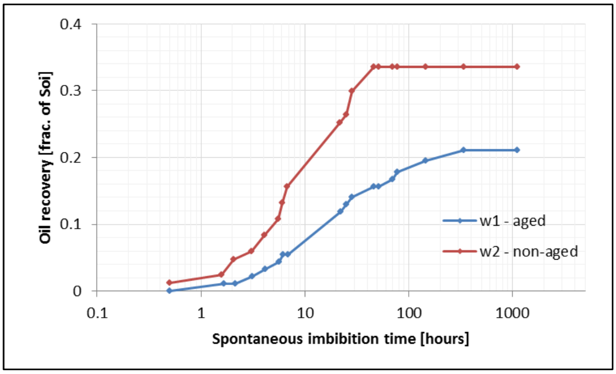

Figure 6.6 – Imbibition characteristics for Berea sandstone. w1 (blue curve) is aged for 14 days at 110 ˚C. w2 (red curve) is not aged at elevated temperature.

I_w ranges from 0.3 to 0.4 for neutral to weakly water-wet systems whereas strongly water-wet systems are at, or very close to unity [78]. I_w for w1 is 0.42 which can be characterized as weakly water-wet. Most of the oil that was produced in total was produced during the forced displacement process. For w2 on the other hand, I_w is 1, thus no oil was produced during the same process and the core can be characterized as strongly water-wet.

This test confirmed that we were able to shift the wettability of the cores from the natural strongly water-wet state to a less water-wet state using the aging method described in chapter 5.4.

6.2.3 Heterogeneities

The core samples used in this work, Berea sandstone cores, are often characterized to be homogeneous. However, visual inspection of the core samples revealed laminations across some of them, see the photograph in Figure 6.7.

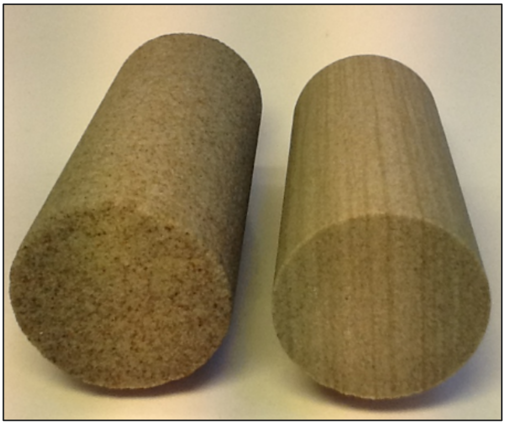

Figure 6.7 - Photograph of two Berea core samples, homogeneous to the left and laminated to the right.

To better characterize them, images from optical microscope were taken of thin sections at different areas on the same rock with visual laminations, Figure 6.8. The left image represents the host rock which is the largest part of the rock. The right image is one type of compaction band present with somewhat lower porosity and permeability than the host rock.

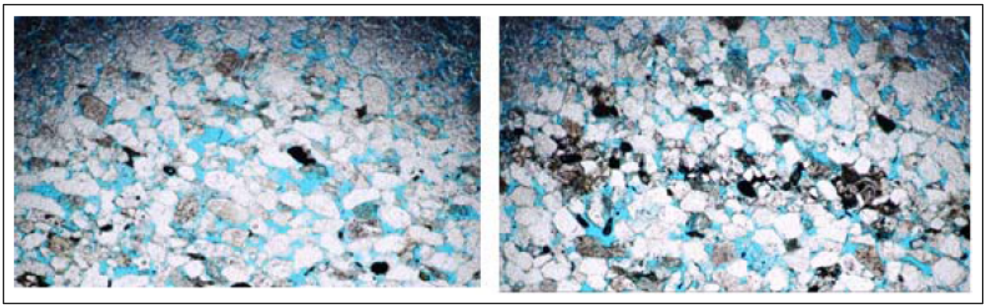

Figure 6.8 - Optical microscope image of homogeneous part of core sample (left), and laminated part (right).

Dispersion tests were carried out on most of the cores in this work to understand their flow properties and to see if there were any differences between the homogeneous and heterogeneous cores. The tests were carried out both at S_{or} and in clean state (100 % water saturated). Figure 6.9 and Figure 6.10 shows dispersion profiles for core A1 (visually homogeneous) and core B (visually heterogeneous) from P1, and core L1 (visually heterogeneous) and H1 (visually homogeneous) from P2 respectively.

The dispersion curves for the homogeneous cores (A1 and H1) display close to ideal dispersion behavior in the two states, indicating that the residual oil distribution does not give rise to an increased number of isolated pores.

Larger differences are observed when comparing the dispersion profiles in clean state and at S_{or} for the heterogeneous cores (B and L1). At S_{or} they break through earlier than what would be expected for a homogeneous core, indicating the presence of isolated pores that do not contribute to flow. In clean state the curves shift towards the right, i.e. there is an increase in effective pore volume. This can be understood in terms of wettability and pore occupancies. In an oil-wet porous medium, water will first enter the large pores, i.e. the high permeable zones. As a consequence, residual oil is found in the low permeable laminas, which are not contributing to the flow of water during the dispersion measurements. When the core is cleaned, wettability is shifted towards more water-wet, and water will now preferentially enter the small pores associated with the highest capillary pressure. Thus, in the cleaned state the core has a higher effective pore volume with less isolated pores than at $S_{or.}$

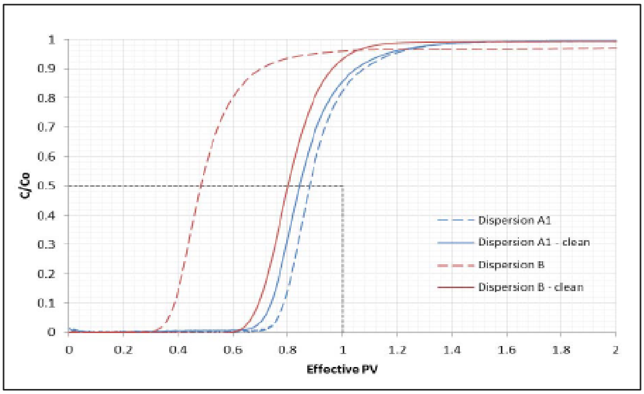

Figure 6.9 - Dispersion curves for core A1 (blue) and B (red) at S_{or} and S_w=1, from P1. The fractional flow of water is plotted against the effective PV, i.e. PV corrected for the presence of residual oil.

In core L1 both profiles break through early, indicating the presence of isolated pores both at S_{or} and in clean state. The profile becomes asymmetrical after cleaning the core which may be due to that removal of residual oil opens up dead-end pores causing tailing of the profile due to mass exchange with these pores.

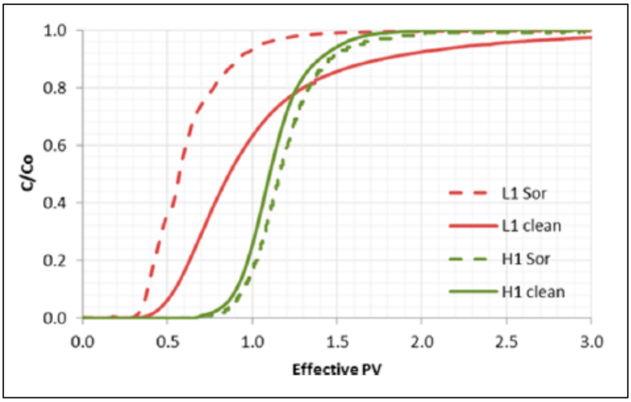

Figure 6.10 - Dispersion curves for core L1 (red) and H1 (green) at S_{or} and S_w=1, from P2. The fractional flow of water is plotted against the effective PV, i.e. PV corrected for the presence of residual oil.

The core material analysis by dispersion measurements can help interpret the results from the flooding experiments. In P2, identical core procedures followed in cores L1 and L3, but the results were not reproducible. This may be a result of the laminations in the cores and address the problem of reproducibility in heterogeneous core material.

6.2.4 Dynamic Retention

During a surfactant flood in an oil containing core, retention mechanisms include adsorption on the mineral surface, precipitation of surfactant, and surfactant partitioning into the oil phase. Retention is an important factor when evaluating a surfactant flood as a high degree of surfactant loss can make the process uneconomical [33]. Since high surfactant retention often is associated with high brine salinity, surfactant in a LS environment is a positive combination in terms of retention. In a dynamic retention experiment in an oil free core, such as in cores R1 and R2 below, the last mechanism above is excluded.

Table 6.4 shows the retention data for R1 and R2 in addition to the retention data for the core flooding experiments in P2 as a supplement. All OS core floods display a higher retention than the LS core floods. Average retention is 0.39 mg surfactant/g rock for the OS floods and 0.24 mg surfactant/g rock for the LS floods. This verifies that retention increases with increasing salinity [33]. Surfactant retention is higher during flow through a 100% water saturated core than during flow at S_{or} in all experiments. One possible explanation for the lower retention values during flow at S_{or} could be oil occupying adsorption sites on the rock surface and thus making less sites available for surfactant adsorption.

Table 6.4 – Retention data for cores R1, R2, L1, L2, L3, H1 and H2

	LSS				OSS		
Core ID	**R1**	**L1**	**L3**	**H1**	**R2**	**L2**	**H2**
Surfactant injected [mg]	206	129	165	164	269	189	161
Surfactant recovered [mg]	143	88	109	104	161	106	76
Surfactant retention [mg]	63	41	56	6	108	82	85
Retention [mg/g]	**0.28**	**0.17**	**0.24**	**0.26**	**0.45**	**0.35**	**0.36**

Figure 6.11 shows effluent surfactant concentration as a function of injected volume for R1 (LS saturated flooded with LSS solution) and R2 (OS saturated flooded with OSS solution). Indications of higher retention in R2 than R1 by later surfactant break through and smaller area under the curve was confirmed by the surfactant concentration measurements showing retentions of 0.28 mg surfactant per gram of rock in R1, and 0.45 mg/g in R2. See Table 6.4.

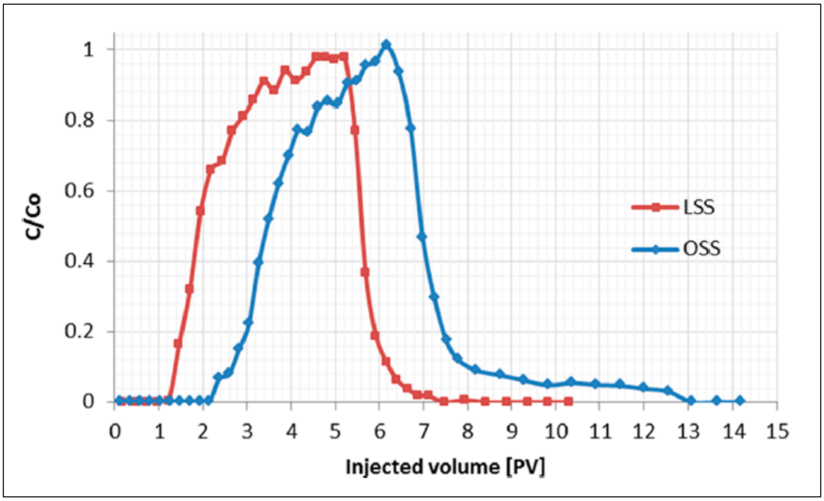

Figure 6.11 – Retention profiles showing normalised produced surfactant concentration as a function of PV injected for core R1, red curve, and R2, blue curve.

6.3 LS Waterflooding at Reduced Capillarity under Different Wettability Conditions (P1)

6.3.1 LSS Injection in Water-Wet Core Sample

It is evident from most LS studies [51] that increased oil recovery by LS water injection are shown using core samples that are in a wetting state other than strongly water-wet. As discussed in chapter 6.2.2, the cores in this work were therefore aged in order to obtain a wettability state other than strongly water-wet.

However, core A2 in P1 was aged at 90°C as opposed to 110°C which was the temperature used for all the other cores in this work. The production results from A2 deviates somewhat from the other cores, and analysing the data indicates that this core possible was in a water-wet state during the flooding experiment. The indications were:

- No additional oil was produced after water break through (WBT) during the first injection step of SW injection. A production profile with no two-phase production following WBT is usually associated with water-wet porous media. By comparison, the other cores in this thesis that were subjected to 110°C during aging, showed significant two-phase production after WBT.
- Strongly water-wet porous media is often associated with a lower oil recovery after water injection than those of a less water-wet state. No other core shows a lower oil recovery than A2 after the first injection step (S_{orw} = 0.35).
- The relative permeability to oil $k_{o\ (Swi)}$ was measured before and after the aging process. In almost all of the cores where these measurements were conducted, the $k_{o\ (Swi)}$ after aging was reduced by 50% or more than $k_{o\ (Swi)}$ before aging. The difference in relative permeability measurements before and after aging for core A2 is smaller than for the other cores.
- Injection of LS brine alone into core A2, did not recovery any additional oil, but an increase in the pressure drop over the core was observed after 2 – 3 PVs LS brine injected, similar to the observations during the C_{sc} experiment, chapter 6.2.1 and Figure 6.5. It is believed to be due to the release of fines (clay) from the rock which was observed in the C_{sc} experiment. This might be an effect in water-wet rock when oil layers are not situated along the pore walls.

Despite that core A2 was flooded with the highest surfactant concentration (1 wt%) yielding the lowest IFT, see chapter 6.1.1, the recovery did not increase beyond what was observed in the experiment where the lowest surfactant concentration (0.2 wt%) yielding the highest IFT. This could be due to the water-wet property of core A2. In a water-wet situation, more of the residual oil will be present as snap-off oil. In a more intermediate-wet situation, however, more residual oil will be in the form of oil layers adhering to the pore walls. The latter is a less stable condition and the interactions between the oil and the pore wall is likely more easily affected by changes in the brine salinity. As a result, this situation may benefit more from the combined LSS effect than a more water-wet situation dominated by snap-off residual oil. A similar observation was made by Alagic et al. [79] in a study involving aged and unaged Berea.

6.3.2 How Low IFT is Necessary to Fully Exploit the Combined LSS Effect?

Surfactant solutions with different IFT values were tested to investigate to which extent the capillary forces needed to be reduced to take advantage of the increased recovery by combining these methods. IFT measurements using the S13 surfactant showed a decreasing IFT with increasing surfactant concentration from 0.2 wt% to 1 wt% corresponding to an IFT of 0.015 mN/m to 5 x 10^{-4} mN/m respectively, see chapter 6.1.1 and Figure 6.1.

Starting with the lowest surfactant concentration, i.e. the highest IFT, in tertiary mode mobilised and produced the whole potential in this core leaving a S_{orLSS} of 0.07. This lead to the conclusion that IFTs in the 10^{-2} mN/m range may be enough in the combined LSS process to produce large amounts of the oil potential in a homogeneous intermediate-wet rock.

6.4 Is LSS waterflooding at moderate IFTs as efficient as OSS waterflooding at ultralow IFTs? (P2)

In order to quantify the effect of using LS water as injection fluid over regular high salinity injection fluid, the oil recovery in a low salinity surfactant (LSS) process at moderately low IFT's was compared to that of a more traditional surfactant flooding process i.e. an optimal salinity surfactant (OSS) process at ultralow IFT.

Thus, as discussed in chapter 6.1.2, phase behavior studies were conducted to find a surfactant formulation which could show ultralow IFT at a salinity too high for a LS effect to be expected, and at the same time show low, but not ultralow, IFT at a salinity considered to be in the LS region.

The surfactant system of APS and IOS was used in all core flooding experiments in tertiary mode in this paper. LSS conditions (salinity of 2500 ppm SW) were used in the three cores, L1, L3 and H1, and OSS conditions (salinity of 15 500 ppm SW) were used in the two cores, L2 and H2. The naming L and H refer to low- and high-permeable core material respectively. Production data for these cores are summarized in Table 6.5.

Table 6.5 – Summary of N_c, recoveries and S_{or} after tertiary surfactant injection for cores L1, L2, L3, H1 and H2.

	LS brine [2500 ppm]			**OS brine [15 500 ppm]**	
Core ID	**L1**	**L3**	**H1**	**L2**	**H2**
N_c (LSS/OSS)	2.4×10^{-4}	2.4×10^{-4}	2.0×10^{-4}	1.5×10^{-2}	1.3×10^{-2}
LSS/OSS recovery [% OOIP]	84.0	85.9	90.3	85.2	92.4
S_{or} (LSS/OSS)	0.10	0.10	0.07	0.10	0.05
ΔS_o (LSS/OSS)	0.06	0.17	0.21	0.16	0.25
S_{or} (LSS/OSS) /S_{or} (LS/OS)	0.63	0.37	0.25	0.38	0.17

S_{or} after surfactant floods reaches values ≤ 0.1 in all cores independent of flooding procedure. The lowest S_{or} were obtained for the high permeable cores, H1 and H2, with the absolute lowest in core H2, which was flooded at optimal salinity with the lowest IFT in these experiments (3 x 10^{-4} mN/m).

The surfactant floods in L1, L3, and H1 were all in the LS regime with a moderate reduction in IFT (0.02 mN/m). Normalized S_{or}, i.e. $S_{or(LSS)}/S_{or(LS)}$, for L3 and H1 were 0.37 and 0.25, respectively. In both cases, the oil recoveries are significantly higher than what would be predicted from capillary desaturation curves (CDC) measured on Berea cores [9]. This increase in recovery above what is expected from a CDC is attributed to the combined effect of low salinity and surfactant (LSS). Even though oil production during LS injection is marginal, oil may nonetheless be redistributed and/or oil layers may be destabilised due to changes in crude oil/brine/rock interactions taking place during LS injection. Redistribution of oil is less likely to occur in cores L1, L3, and H1 as there is little response on the differential pressures during LS injection. Still, even with a moderate reduction in IFT, such as in the LSS flooding experiments in this study, oil layer destabilization coupled with reduced capillarity may give rise to added recovery beyond what would be expected by the action of the surfactant alone.

The N_c's during the OSS flood in L2 and H2 are around 2 orders of magnitude higher than during the LSS flood in L1, L3, and H1. However, the final recoveries and S_{or} are more or less equal, highlighting the combined effect of LSS.

6.5 Is There a Combined Effect of IFT Reduction and Low Salinity on Oil Recovery Compared to That From Lowering IFT Alone? (P3)

In the previous section, chapter 6.4, the results on oil recovery from LSS and OSS injection processes in tertiary mode were compared. Another way of investigating the combined LSS effect is to compare the LSS process with a surfactant process with a sole reduction in IFT. Here, both surfactant systems are in the Winsor I regime giving a moderate reduction in IFT, but only one of the systems are in the LS region.

The salinity difference between the LS and HS brine and the use of different crude oils, requested different surfactant systems for each of the cores in order to stay in the Winsor I microemulsion regime giving rise to a moderate reduction in IFT, see Table 6.2.

Continuous injection of surfactant solution for several pore volumes do not represent real life field projects. The most common way of implementing an EOR surfactant process, is thorough slug injection followed by polymer support. In the following core flooding experiments, 0.5 wt% surfactant slugs were therefore used for the tertiary injection processes, followed by polymer support with a viscosity of close to 10 cP. In-situ saturation monitoring allowed detection of residual oil within the core at different time steps during the injection process, which again, allowed for investigation of the sweep of the tertiary processes. The experiment in core HS1 was not carried out with in-situ saturation monitoring.

Figure 6.12 shows the oil saturation distribution detected by the in-situ scanner as a function of the normalized core length for cores LS1, LS2, and HS2 respectively, initially at S_{oi} (grey), after secondary brine injection at S_{orw} (red) and after tertiary chemical flood at S_{orc} (green). Oil is evenly distributed in the core after primary drainage in all experiments, see the grey curves in Figure 6.12. Further, no holdup of the oil phase at the core outlet during waterflood is observed, see the red curves in Figure 6.12; i.e. there are no indications of capillary end effects.

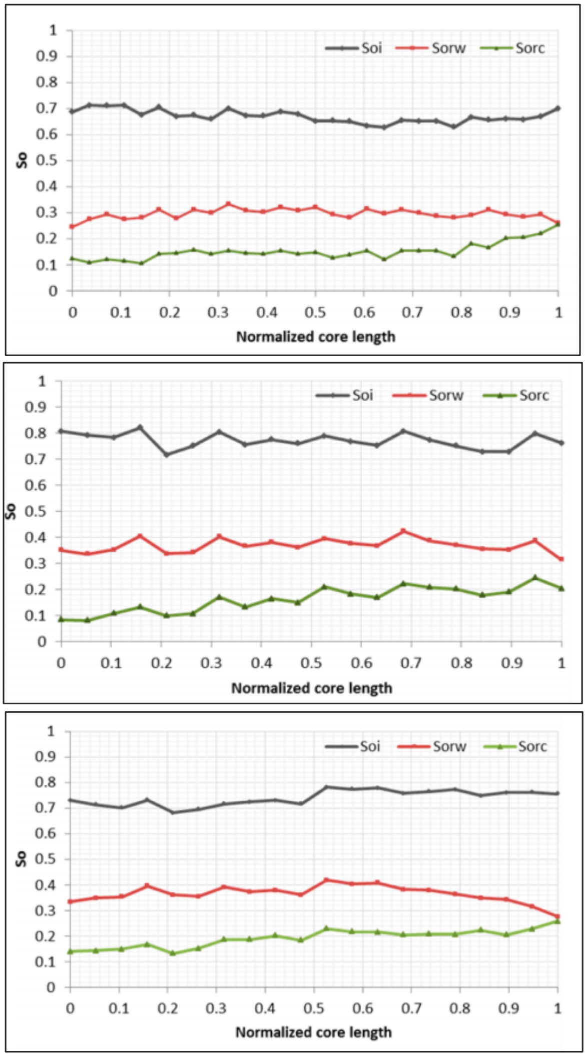

Figure 6.12 – Oil saturation as a function of the normalised core length at S_{oi}, S_{orw} and S_{orc} for core LS1, LS2 and HS2 going from top to bottom respectively.

6.5.1 Tertiary Surfactant Injection

Figure 6.13 shows oil saturation as a function of the normalized core length obtained from the in-situ saturation measurements during the 0.5 PV surfactant slug injections for cores LS1, LS2, and HS2, respectively. The yellow curves, are the oil distribution after waterflooding at $S_{orw,}$ and the green curves are the oil distribution after injection of the surfactant slug. During injection of the surfactant slug, the oil saturation distribution inside the cores changes showing that it propagates towards the outlet.

By the end of the surfactant injection process the surfactant slug is expected to have covered the adsorption capacity near the core inlet. The effect of this process on oil mobilization can be therefore be studied by comparing the saturation near the core inlets.

The LSS process in core LS1 reduces the S_o at the core inlet by 5 saturation units with an IFT of 0.12 mN/m. Compared to LS1, the IFT in LS2 was reduced by a factor of 5 (IFT = 0.025 mN/m) which reduced the S_o at the core inlet by 24 saturation units during the LSS slug process. Picking up the discussion in chapter 6.3.2 on how low IFT is needed to take advantage of the combined process, it seems that using an IFT in the 10^{-1} like for LS1 still leaves an oil potential to be recovered.

The IFT of the surfactant slug in core HS2 using HS water, showed the lowest IFT in P3, i.e., 0.015 mN/m. The oil saturation near the core inlet decreases by 18 saturation units after injection of the HSS slug. Although the IFT was lower here than in the LSS experiment in core LS2, the oil saturation was 6 units higher at the end of the surfactant flood.

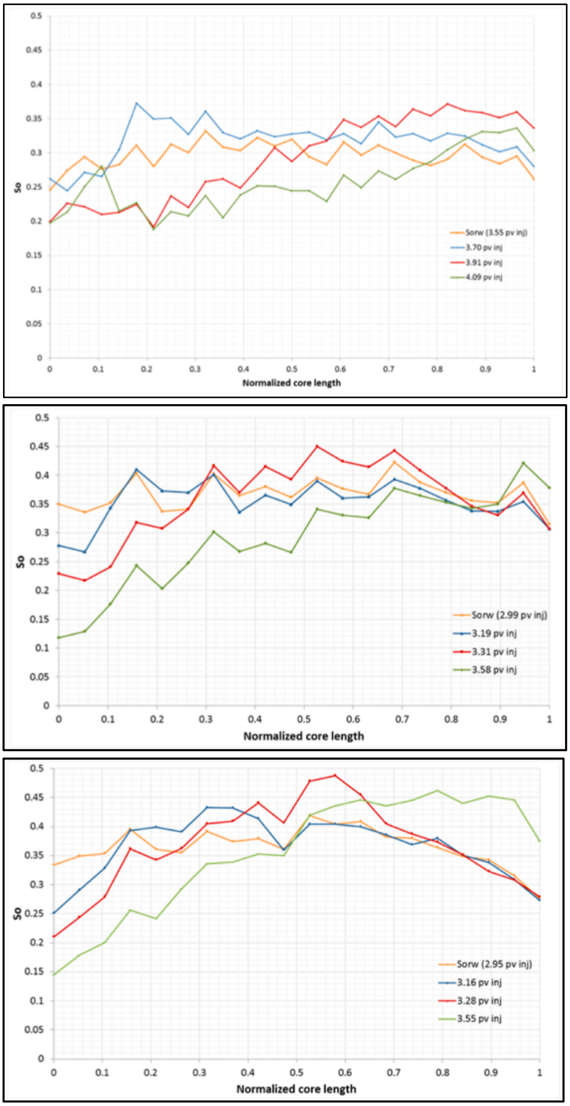

Figure 6.13 – In situ oil saturation development during surfactant slug injection in cores LS1, LS2 and HS2 going from top to bottom respectively.

6.5.2 Tertiary Polymer Injection

Injection of polymer solution followed the 0.5 PV surfactant slugs in all cores. A closer look at the S_{orc} (residual oil after chemical injection) curve in each experiment, Figure 6.14, reveals that the surfactant slugs were too small to mobilise oil equally across the core, if we assume that the polymer only works as a pressure drive. The S_{orc} curves (purple curves in Figure 6.14) gradually increase from the core inlet to outlet, leaving higher oil saturations at the core ends.

A closer look at the tertiary injection process in core LS1 the small oil bank developed is reflected by the moderate oil recovery. The viscoelastic property of the polymer solution reduces the oil saturation at the core inlet further by 3 saturation units in this core.

In cores LS2 and HS2 on the other hand, the oil saturation of the first 0.15 PV of the core length has reached S_{orc} during the surfactant injection; i.e., the surfactant has effectively mobilized and displaced oil here. From 0.15 PV of the core length and toward the outlet, the polymer sweeps the oil solubilized by the surfactant slug. If the surfactant slugs had been larger, the average S_{orc} could possibly be equal to S_{orc} reached near the core inlets. For instance, would S_{orc} in LS2 reach a value of 0.1, instead of 0.18? A S_{orc} value of 0.1 in LS2 would be in line with previous experiments reported for LSS experiments with continuous surfactant injection with the same reduction in IFT [28].

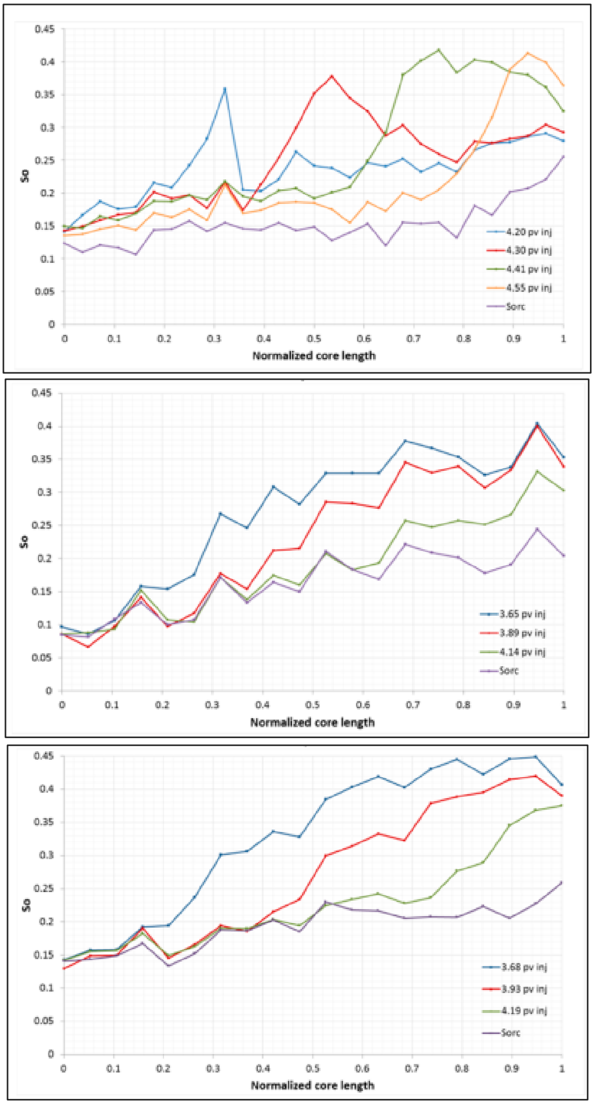

Figure 6.14 - In situ oil saturation development during polymer injection in cores LS1, LS2 and HS2 going from top to bottom respectively.

The gradual increase in residual oil across the cores (S_{orc}) leads to the conclusion that the surfactant slug contained an insufficient amount of surfactant to mobilise oil at the core outlet to the same extent as the core inlet. With a continuous surfactant injection strategy, a lower average S_{orc} similar to S_{orc} at the core inlet would likely be obtained.

Since the IFT in these experiments are different it is difficult to evaluate the effect of LSS injection based solely on oil recovery. The N_c and the CDC curve in the next chapter, however, gives the relationship between the residual oil and the IFT.

6.5.3 Capillary Number, Nc

N_c values for the tertiary processes discussed in chapter 6.5.1 and 6.5.2 (cores LS1, LS2, HS1 and HS2), are calculated using the polymer viscosity and surfactant solution to crude oil IFT.

The capillary number, N_c, increases in the order LS1 < HS1 < LS2 < HS2, increasing by a factor of roughly 10 from LS1 to HS2. Assuming that the critical capillary number, N_{cc}, is reached, S_{or} should decrease in the reverse order, i.e., with the highest N_c (HS2) giving rise to the lowest S_{or}, according to typical capillary desaturation behavior [4,80,81]. CDC data from the HSS and LSS experiments seem to follow two different curves, see Figure 6.15, with the surfactant flooding experiments in a LS environment giving rise to lower residual oil saturations at slightly lower N_c. This may be an indication of a combined effect of IFT reduction and LS on recovery compared that from a reduction in IFT alone.

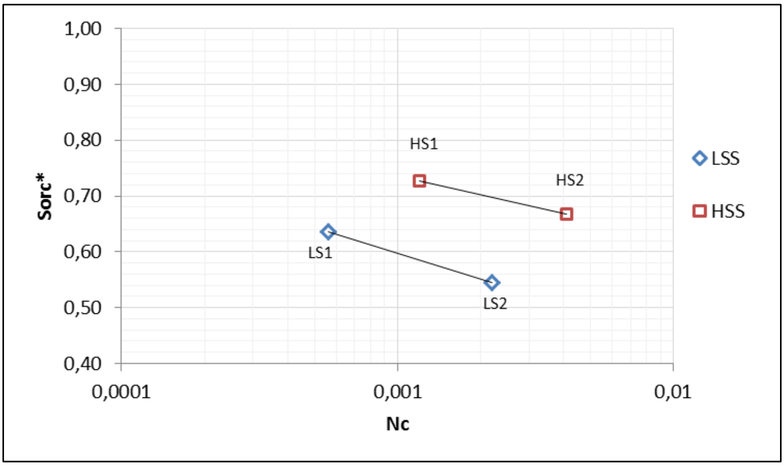

Figure 6.15 – S_{orc}* as a function of N_c for the tertiary flooding procedure for the four cores in P3.

7. CONCLUDING REMARKS

The work in this thesis have focused on the hybrid EOR technique of combining low salinity injection with surfactant (LSS), and investigate whether these two techniques are more efficient combined than either of the two processes applied alone. This section summarizes the most important observations from this work.

- Low Salinity and Surfactant Flooding in Winsor I systems

No additional oil was produced during tertiary LS water injection alone. Oil may nonetheless be destabilized and/or redistributed due to changes in the crude oil/brine/rock interactions taking place during LS injection. Speculations have been made whether the tertiary low salinity injection often show no, or moderate effect due to the absence of a continuous oil film. It has also been suggested that the repulsive forces caused by LS water that thickens the water films and destabilizes oil layers are not strong enough for the oil to be mobilized by the imposed flow [47].

Winsor I phase behavior systems are generally formed at low salinities. A surfactant flood in a Winsor I environment is thought to be the simplest type and straightforward because the surfactant is transported and remains in the aqueous phase [5] and the systems conditions exists throughout the flood. The drawback of this design has been that the moderate reduction in IFT in these systems are usually not low enough for good oil displacement [37].

We showed that by taking advantage of the destabilized oil by LS water, and combining it with Winsor I surfactant flooding experiments with a moderate reduction in IFT in the 10^{-2} mN/m area, we obtained comparable recoveries to traditional surfactant flooding experiments operating in the ultralow IFT regime (10^{-4} mN/m). Surfactant systems at moderate IFT´s are easier to obtain, exists over a wider range and require thus less effort to control than traditional surfactant flooding processes with ultralow IFT.

Chemical loss is a key factor for economical evaluation of a surfactant flood and should be minimized. Retention is lower in surfactant floods performed at lower salinities since adsorption increases with increasing salinity, and precipitation and phase trapping of the surfactant is more likely to occur at higher salinities. In this work, the retention was lower in the LSS experiments compared to the experiments using higher salinities. Retention was measured in the range of 0.17 – 0.28 mg/g for the LSS experiments and 0.35 – 0.45 mg/g in the HSS/OSS experiments. For higher salinities, like SW salinities, retention has been measured to be around 0.9 mg/g in Berea sandstone cores [82].

- Evalutaion of the Capillary Number (N_c) for the different flooding strategies

The Capillary Desaturation Curve (CDC) is a tool often used to predict microscopic displacement efficiency [80], and can serve as an estimate for the amount of residual oil that can be achieved under given pressure gradients and capillary forces. Thus, the capillary number (N_c) has been an important parameter in this work in order to quantify the efficiency of the different core flooding experiments and thereby compare them and investigate if there is an added benefit from the LSS process as compared to a regular surfactant injection process.

Figure 7.1 shows the CDC plots (N_c as a function of S_{or}) after the tertiary surfactant flood for the main cores. Blue symbols represent LSS experiments with a moderate reduction in IFT, green symbols represent high salinity surfactant experiments at ultralow IFTs (OSS) and red symbols represent high salinity surfactant experiments with a moderate reduction in IFT (HSS). Filled points represent the continuous surfactant injection strategy, while points without fill represent surfactant slug injection strategy.

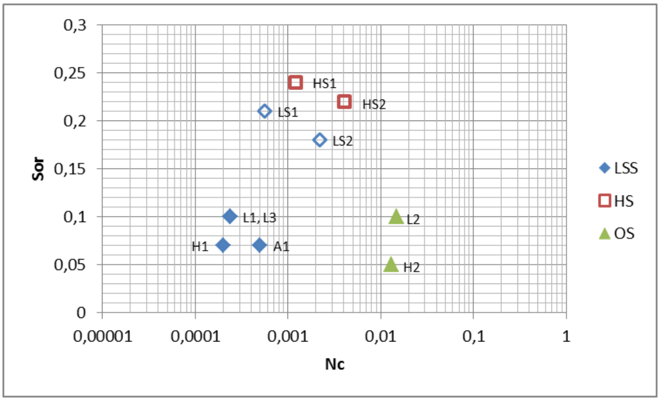

Figure 7.1 - S_{or} as a function of N_c for the tertiary flooding procedure for the main cores in this work. Points without fill indicate surfactant slug experiments.

The oil recoveries from the LSS experiments (filled blue points) are significantly higher than what would be predicted from capillary desaturation curves (CDC) measured on Berea cores [9]. The CDC in Figure 2.1 (based on CDC from the literature) suggests a S_{or} between 20 - 25 % at these N_c´s. This increase in recovery above what is expected from a CDC is attributed to the combined effect of low salinity and surfactant (LSS).

The N_c’s during the OSS floods in L2 and H2 (green points in Figure 7.1) give oil recoveries in line with what would be expected by the N_c relationship. Even though the IFT´s used here are 60 times lower and the N_c´s are around 2 orders of magnitude higher than during the LSS floods in L1, L3, and H1, the final recoveries and S_{or} are more or less equal, highlighting the combined effect of LSS.

Even though the mechanisms behind the LSE alone is not proven in this work or in other LS studies, the mechanisms that are suggested imply that oil layers may be destabilized due to changes in crude oil/brine/rock interactions taking place during LS injection. With only a moderate reduction in IFT, such as in the LSS flooding experiments in this study, coupled with this mechanism give rise to added recovery beyond what is expected by the action of Winsor I surfactant systems alone.

- Core characterization

The complexity and variety of crude oil/brine/rock interactions present in the literature are often highlighted as one of the main difficulties when investigating the mechanisms behind the Low Salinity Effect. Knowledge about the properties of the materials (e.g. wettability, flow properties and water sensitivity) used are therefore important.

Comparing the LSS flooding results between a water-wet core and the mixed-wet cores in this work indicates that the LSS injection process yields higher oil recoveries and a more efficient process when the core is aged to obtain a mixed-wet condition. Higher recoveries in mixed-wet core material are attributed to destabilization of adsorbed oil layers which are mobilized and produced due to a moderate reduction in the IFT.

The Critical Salt Concentration (CSC) experiments showed that the core material used in this work is sensitive to LS brine injection by an increase in differential pressure over the core with decreasing salinity, and observation of clay particles in the effluent when distilled water was injected. The DLVO theory can explain the mechanism for fines mobilization and is also a suggested mechanism for the LSE. Upon injection of LS brine in the CSC experiment, the electrical double layer in the aqueous phase between rock particles will expand and the tendency for stripping of fines is increased. Explaining the LSE, the water film between the rock and the oil becomes thicker upon injection of LS brine due to expansion of the electrical double layer between rock/brine and oil/brine resulting in destabilization and/or mobilization of the oil adhered to the rock thus leading to a more water-wet rock.

The core material analysis by dispersion measurements can help interpret the results from the flooding experiments. In P2, identical core preparations and flooding sequences were performed on cores L1 and L3, yet the production data in these experiments showed large variations. This may be a result of the laminations in the cores and address the problem of reproducibility in heterogeneous core material.

8. FURTHER WORK

This thesis builds on the hypothesis that oil layers adhered to rock surface are destabilized by low salinity injection. However, the work has not concentrated on experiments to investigate the mechanism(s) behind this effect alone. This is a topic many researchers have been trying to find more precise answers to for years, and lately it seems to be a growing interest towards the theories concerning thin liquid films between crude oil/brine and rock/brine surfaces. It would be interesting to follow this and measure brine film thickness as an effect of brine salinity. One method is by Ellipsometry. Another method for this purpose is measurements of the Zeta potential.

In this work, we have investigated and compared the oil recovery from LSS surfactant systems to other surfactant systems like; a high salinity system in a Winsor I regime using slug injection strategy and high salinity system in Winsor III regime using continuous injection strategy. Due to the different strategies (continuous vs slug injection), the results showed different trends in the CDC plot. Performing continuous flooding strategy on all the different surfactant systems and then later on optimize them for slug injection would obtain comparable experiments for all the systems and strategies used.

From the core flooding results, it seems like the CDC follow different trends for the LSS experiments compared to the HSS/OSS experiments. A series of core flooding experiments where the IFT is gradually reduced in both the LSS regime and the HSS regime would give complete CDC for the two processes. That way we could conclude if the two processes show different trend over the whole range of N_c's.

Performing LS and LSS flooding experiments on core samples while using micro-CT scanning would obtain saturations on pore level. This could give more precise answers to e.g. the wettability alteration theory by LS injection or the hypothesis of less trapping of destabilized oil when LS injection is used together with surfactant.

REFERENCES

[1] Council, W. E. (2013) *World Energy Scenarios - Composing energy futures to 2050*.

[2] OPEC. (2016) *World Oil Outlook*.

[3] Craig Jr, F. F. (1971) *The Reservoir Engineering Aspects of Waterflooding*. Texas: Monograph Series, SPE Vol 3.

[4] Taber, J. J. (1969) *Dynamic and Static Forces Required To Remove a Discontinuous Oil Phase from Porous Media Containing Both Oil and Water*. SPE J. 9, 1: 3-12.

[5] Hirasaki, G. J., van Domselaar, H. R. and Nelson, R. C. (1983) *Evaluation of the Salinity Gradient Concept in Surfactant Flooding*. Soc. Petr. Eng. 23, 03.

[6] Flaaten, A. K., Nguyen, Q. P., Pope, G. A. and Zhang, J. A. (2009) *A Systematic Laboratory Approach to Low-Cost, High-Performance Chemical Flooding*. SPE Res. Eval. & Eng. 12, 5: 713-723.

[7] Larson, R. G., Davis, H. T. and Scriven, L. E. (1980) *Displacement of Residual Nonwetting Fluid From Porous Media* Chemical Engineering Science 36: 75-85.

[8] Chatzis, I. and Morrow, N. R. (1984) *Correlation of Capillary Number Relationships for Sandstone*. SPE J. 24, 5: 555-562.

[9] Garnes, J. M., Mathisen, A. M., Scheie, A. and Skauge, A. (1990) *Capillary Number Relations for Some North Sea Reservoir Sandstones*. SPE/DOE 20264 Presented at the Seventh Symposium on Enhanced Oil Recovery, April 22-25, Tulsa, Oklahoma.

[10] Abrams, A. (1975) *The Influence of Fluid Viscosity, Interfacial Tension, and Flow Velocity on Residual Oil Saturation Left by Waterflood*. Soc. Petr. Eng. 15, 5: 437-447.

[11] Stegemeier, G. L. (1974) *Realtionship of Trapped Oil Saturation to Petrophysical Properties of Porous Media*. Presented at SPE Improved Oil Recovery Symposium, 22-24 April, Tulsa, Oklahoma.

[12] Mohanty, K. K. and Salter, S. J. (1983) *Multiphase Flow in Porous Media: III. Oil Mobilization, Transverse Dispersion, and Wettability*. Soc. Petr. Eng. Presented at the 58th Annual Technical Conference and Exhibition in San Fransisco, October 5-8

[13] Cense, A. W. and Berg, S. (2009) *The Viscous-Capillary Paradox In 2-Phase Flow In Porous Media*. Presented at the International Symposium of the Society of Core Analysts in Noordwijk, 27-30 September, The Netherlands.

[14] Shiran, B. S. and Skauge, A. (2013) *Enhanced Oil Reocvery (EOR) by Combined Low Salinity Water/Polymer Flooding*. Energy & Fuels 27, 03: 1223-1235.

[15] Mohammadi, H. and Jerauld, G. (2012) *Mechanistic Modeling of the Benefit of Combining Polymer with Low Salinity Water for Enhanced Oil Recovery*. Soc. Petr. Eng. SPE Improved Oil Recovery Symposium, 14-18 April, Tulsa, Oklahoma.

[16] Dang, C. T. Q. (2015) *Mechanistic Modeling, Design, and Optimization of Low Salinity Waterflooding*. PhD Thesis University of Calgary.

[17] Winsor, P. A. (1968) *Binary and Multicomponent Solutions of Amphiphilic Compounds. Solubilization and the Formation, Structure and Theoretical Significance of Liquid Crystalline Solutions*. Chemical Reviews 68, 1.

[18] Schulman, J. H., Stoeckenius, W. and Prince, L. M. (1959) *Mechanism of Formation and Structure of Micro Emulsions by Electron Microscopy*. J. Phys. Chem. 63: 1677-1680.

[19] Healy, R. N. and Reed, R. L. (1974) *Physicochemical aspects of microemulsion flooding*. SPE J. 257, Trans: 491-501.

[20] Winsor, P. A. (1948) *Solvent Properties of Amphiphilic Compounds*. Trans. Faraday Soc. 44: 376.

[21] Healy, R. N., Reed, R. L. and Stenmark, D. G. (1976) *Multiphase Microemulsion Systems*. SPE J. 16, 3: 147-160.

[22] Berg, J. C. (2010) *An Introduction to Interfaces & Colloids - The Bridge to Nanoscience*. World Scientific Publishing Co. Pte. Ltd.

[23] Salager, J. L., Morgan, J. C., Schechter, R. S., Wade, W. H. and Vasquez, E. (1979) *Optimum Formulation of Surfactant/Water/Oil Systems for Minimum Interfacial Tension or Phase Behavior*. SPE J. 19, 2: 107-115.

[24] Aarra, M. G., Høiland, H. and Skauge, A. (1999) *Phase Behavior and Salt Partitioning in Two- and Three-Phase Anionic Surfactant Microemulsion Systems: Part 1, Phase Behavior as a Function of Temperature*. J. Colloid Interf. Sci 215: 201-215.

[25] Kahlweit, M., Strey, R. and Busse, G. (1990) *Effect of Alcohols on the Phase Behavior of Microemulsions*. J. Phys. Chem. 95: 5344-5352.

[26] Salter, S. J. (1977) *The Influence of Type and Amount of Alcohol on Surfactant-Oil-Brine Phase Behavior and Properties*. SPE Presented at the SPE Annual Fall Technical Conference and Exhibition, 9-12 October, Denver, Colorado.

[27] Wade, W. H., Morgan, J. C., Schechter, R. S., Jacobson, J. K. and Salager, J. L. (1978) *Interfacial Tension and Phase Behavior of Surfactant Systems*. J. Pet. Sci. Eng. 18, 4: 242-252.

[28] Johannessen, A. M. and Spildo, K. (2013) *Enhanced Oil Recovery (EOR) by Combining Surfactant with Low Salinity Injection*. Energy & Fuels 27, 10: 5738-5749.

[29] Tien, T. H. and Bettahar, M. (2000) *Effect of the Water-Oil Ratio on Brine-Surfactant-Alcohol-Oil Systems Optimized for Soil Remediation*. J Mater Cycles Waste Manag 2: 109-117.

[30] Pashley, R. M. and Karaman, M. E. (2007) *Applied Colloid and Surface Chemistry*. John Wiley & Sons Ltd.

[31] Huh, C. (1979) *Interfacial Tension and Solubilizing Ability of a Microemulsion Phase That Coexists with Oil and Brine*. J. Colloid Interf. Sci. 71, 2: 408-426.

[32] Reed, R. L. and Healy, R. N. (1977) *Some Physicochemical Aspects of Microemulsion Flooding: A Review*. Reprinted from Eds. Academic Press: 383-437.

[33] Glover, C. J., Puerto, M. C., Maerker, J. M. and Sandvik, E. L. (1979) *Surfactant Phase Behavior and Retention in Porous Media*. SPE J. 19, 3: 183-193.

[34] Barnes, J. R., Dirkzwager, H., Smit, J. R., Smit, J. P., On, A., Navarrete, R. C., Ellison, B. H. and Buijse, M. A. (2010) *Application of Internal Olefin Sulfonates and Other Surfactants to EOR. Part 1: Structure - Performance Relationships for Selection at Different Reservoir Conditions*. Soc. Petr. Eng.: Presented at SPE Improved Oil Recovery Symposium, 24-28 April 2010, Tulsa, Oklahoma, USA.

[35] Sahni, V., Dean, R. M., Britton, C., Kim, D. H. and Pope, G. A. (2010) *The Role of Co-Solvents and Co-Surfactants in Making Chemical Floods Robust*. Soc. Petr. Eng. SPE Improved Oil Recovery Symposium, 24-28 April, Tulsa, Oklahoma.

[36] Solairaj, S., Britton, C., Kim, D. H., Weerasooriya, U. and Pope, G. A. (2012) *Measurement and Analysis of Surfactant Retention*. Presented at the SPE Improved Oil Recovery Symposium, Tulsa, 14-18 April, Oklahoma SPE 154247.

[37] Nelson, R. C. (1982) *The Salinity-Requirement Diagram - A Useful Tool in Chemical Flooding Research and Development*. SPE J. 22, 2: 259-270.

[38] Jadhunandan, P. P. and Morrow, N. R. (1991) *Spontaneous Imbibition of Water by Crude Oil/Brine/Rock System*. In Situ 15:4.

[39] Jadhunandan, P. P. and Morrow, N. R. (1995) *Effect of Wettability on Waterflood Recovery for Crude-Oil/Brine/Rock Systems*. SPE 10, 1: 40-46.

[40] Yildiz, H. O. and Morrow, N. R. (1995) *Effect of Brine Composition on Recovery of Moutray Crude Oil by Waterflooding*. J. Pet. Sci. Eng. 14: 159-168.

[41] Tang, G. Q. and Morrow, N. R. (1997) *Salinity, Temperature, Oil Composition and Oil Recovery by Waterflooding*. SPE Res. Eng. 12, 4: 269-276.

[42] Tang, G. Q. and Morrow, N. R. (1999) *Influence of Brine Composition and Fines Migration on Crude Oil/Brine/Rock Interactions and Oil Recovery*. J. Pet. Sci. Eng. 24: 99-111.

[43] Sharma, M. M. and Filoco, P. R. (2000) *Effect of Brine Salinity and Crude-Oil Properties on Oil Recovery and Residual Saturations*. SPE J. 5, 3: 293-300.

[44] McGuire, P. L., Chatham, J. R., Paskvan, F. K., Sommer, D. M. and Carini, F. H. (2005) *Low Salinity Oil Recovery: An Exciting New EOR Opportunity for Alaska's North Slope*. Soc. Petr. Eng. SPE Western Regional Meeting, 30 March-1 April, Irvine, California.

[45] Lager, A., Webb, K. J., Collins, I. R. and Richmond, D. M. (2008) *LoSal$_{TM}$ Enhanced Oil Recovery: Evidence of Enhanced Oil Recovery at the Reservoir Scale*. Presented at SPE Improved Oil Recovery Symposium, 20-23 April, Tulsa, Oklahoma.

[46] Rivet, S. M., Lake, L. W. and Pope, G. A. (2010) *A Coreflood Investigation of Low-Salinity Enhanced Oil Recovery*. Presented at the SPE Annual Technical Conference and Exhibition, 19-22 September, Florence, Italy.

[47] Nasralla, R. A. and Nasr-El-Din, H. A. (2012) *Double-Layer Expansion: Is It A Primary Mechanism of Improved Oil Recovery by Low-Salinity Waterflooding?* Presented at the 18th SPE Improved Oil Recovery Symposium held in Tulsa, Oklahoma, USA, 14.-18. April.

[48] Austad, T., RezaeiDoust, A. and Puntervold, T. (2010) *Chemical Mechanism of Low Salinity Water Flooding in Sandstone Reservoirs*. SPE 129767. Presented at the SPE IOR Symposium held in Tulsa, Oklahoma, USA, 24.-28. April 2010.

[49] Myint, P. C. and Firoozabadi, A. (2015) *Thin Liquid Films in Improved Oil Recovery from Low-Salinity Brine*. Colloid and Interf. Sci. 20: 105-114.

[50] Sheng, J. J. (2014) *Critical Review of Low-Salinity Waterflooding*. J. Pet. Sci. Eng. 120: 216-224.

[51] Morrow, N. R. and Buckley, J. S. (2011) *Improved Oil Recovery by Low-Salinity Waterflooding*. Distinguished Author Series, SPE 129421.

[52] Ligthelm, D. J., Gronsveld, J., Hofman, J. P., Brussee, F., Marcelis, F. and van der Linde, H. A. (2009) *Novel Waterflooding Strategy by Manipulation of Injection Brine Composition*. SPE 119835 Presented at the SPE EUROPEC/EAGE Annual Conference and Exhibition, Amsterdam, The Netherlands, 8-11 June.

[53] Lee, S. Y., Webb, K. J., Collins, I. R., Lager, A., Clarke, S. M., O'Sullivan, M. and Routh, A. F. (2011) *Low Salinity Oil Recovery – Increasing Understanding of the Underlying Mechansims of Double Layer Expansion*. Presented at the 16th European Symposium on Improved Oil Recovery, Cambridge, 12-14 April.

[54] Nasralla, R. A., Bataweel, M. A. and Nasr-El-Din, H. A. (2011) *Investigation of Wettability Alteration by Low Salinity Water in Sandstone Rock* SPE 146322 Presented at the SPE Offshore Europe Oil and Gas Conference and Exhibition, Aberdeen, UK, 6-8 September.

[55] Shaw, D. J. (1969) *Electrophoresis*. London, New Your, Academic Press.

[56] Lager, A., Webb, K. J., Black, C. J. J., Singleton, M. and Sorbie, K. S. (2006) *Low Salinity Oil Recovery - An Experimental Investigation*. Presented at the International Symposium of the Society of Core Analysts in Trondheim, 12-16 September, Norway.

[57] Jones, F. O. (1964) *Influence of Chemical Composition of Water on Clay Blocking of Permeability*. Journal of Petroleum Technology 16, 4: 441-446.

[58] RezaeiDoust, A., Puntervold, T. and Austad, T. (2010) *A Discussion of the Low Salinity EOR Potential for a North Sea Sandstone Field*. Presented at the SPE Annual Technical Conference and Exhibition, 19-22 September, Florence, Italy.

[59] Zhang, Y., Xie, X. and Morrow, N. R. (2007) *Waterflood Performance by Injection of Brine with Different Salinity for Reservoir Cores*. Presented at SPE Annual Technical Conference and Exhibition, 11-14 November, Anaheim, California.

[60] Pu, H., Xie, X., Yin, P. and Morrow, N. R. (2008) *Application of Coalbed Methane Water to Oil Recovery by Low Salinity Waterflooding*. Soc. Petr. Eng. Presented at the SPE/DOE Improved Symposium held in Tulsa, Oklahoma, USA, 19-23 April.

[61] Pope, G. A., Lake, L. W. and Helfferich, F. G. (1978) *Cation Exchange in Chemical Flooding: Part 1 - Basic Theory Without Dispersion*. Soc. Petr. Eng. 18, 6.

[62] Alagic, E. and Skauge, A. (2010) *Combined Low Salinity Brine Injection and Surfactant Flooding in Mixed−Wet Sandstone Cores*. Energy & Fuels 24, 6: 3551-3559.

[63] Graue, A., Aspenes, E., Bognø, T., Moe, R. W. and Ramsdal, J. (2002) *Alteration of Wettability and Wettability Heterogeneity*. J. Petrol. Sci. Eng. 33: 3-17.

[64] Buckley, J. S., Liu, Y. and Monsterleet, S. (1998) *Mechanisms of Wetting Alteration by Crude Oils*. SPE J. 3, 1: 54-61.

[65] Morrow, N. R., Ma, S., Zhou, X. and Zhang, X. (1994) *Characterization of Wettability from Spontaneous Imbibition Measurements*. Petr. Soc. CIM and AOSTRA 47: 1-15.

[66] Coats, K. H. and Smith, B. D. (1964) *Dead-End Pore Volume and Dispersion in Porous Media*. SPE J. 4, 1: 73-84.

[67] Levitt, D. B., Jackson, A. C., Heinson, C., Britton, L. N., Malik, T., Dwarakanath, V. and Pope, G. A. (2009) *Identification and Evaluation of High-Performance EOR Surfactants*. SPE Res. Eng. 12, 2: 243-253.

[68] Hirasaki, G. J., Miller, C. A. and Puerto, M. C. (2008) *Recent Advances in Surfactant EOR*. SPE J. SPE 115386.

[69] Barnes, J. R., Groen, K., On, A., Dubey, S., Reznik, C., Buijse, M. A. and Shepherd, A. G. (2012) *Controlled Hydrophobe Branching to Match Surfactant to Crude Oil Composition for Chemical EOR*. Presented at the SPE Improved Oil Recovery Symposium, Tulsa, 14-18 April, Oklahoma SPE 154084.

[70] Liu, S., Zhang, D. H., Yan, W., Puerto, M. C., Hirasaki, G. J. and Miller, C. A. (2008) *Favorable Attributes of Alkaline-Surfactant-Polymer Flooding*. SPE J. 13, 1: 5-16.

[71] Khilar, K. C. and Fogler, H. S. (1983) *Water Sensitivity of Sandstones*. SPE J. 23, 1: 55-64.

[72] Lever, A. and Dawe, R. A. (1984) *Water-Sensitivity and Migration of Fines in the Hopeman Sandstone*. Journal of Petroleum Geology 7, 1: 97-107.

[73] Kia, S. F., Fogler, H. S. and Reed, M. G. (1987) *Effect of Salt Composition on Clay Release in Berea Sandstones*. SPE Production Engineering 2, 4: 277-283.

[74] Graue, A., Viksund, B. G., Eilertsen, T. and Moe, R. (1999) *Systematic Wettability Alteration by Aging Sandstone and Carbonate Rock in Crude Oil*. J. Petrol. Sci. Eng. 24: 85-97.

[75] Amott, E. (1959) *Observations Relating to the Wettability of Porous Rock*. Trans. AIME 216: 156-162.

[76] Donaldson, E. C., Thomas, R. D. and Lorenz, P. B. (1969) *Wettability Determination and Its Effect on Recovery Efficiency*. SPE 9, 1: 13-20.

[77] Anderson, W. G. (1987) *Wettability Literature Survey Part 5: The Effects of Wettability on Relative Permeability*. SPE 39, 11: 1453-1468.

[78] Morrow, N. R., Lim, H. T. and Ward, J. S. (1986) *Effect of Crude-Oil-Induced Wettability Changes on Oil Recovery*. SPE Formation Evaluation 1, 1: 89-103.

[79] Alagic, E., Spildo, K., Skauge, A. and Solbakken, J. (2011) *Effect of crude oil ageing on low salinity and low salinity surfactant flooding*. Journal of Petroleum Science and Engineering 78, 2: 220-227.

[80] Abeysinghe, K. P., Fjelde, I. and Lohne, A. (2012) *Dependency of Remaining Oil Saturation on Wettability and Capillary Number*. SPE 160883 Presented at the SPE Saudi Arabia Section Technical Symposium and Exhibition, April 8-11.

[81] Delshad, M., Delshad, M., Bhuyan, D., Pope, G. A. and Lake, L. W. (1986) *Effect of Capillary Number on the Residual Saturation of a Three-Phase Micellar Solution*. SPE/DOE 14911 Presented at the Fifth Symposium on Enhanced Oil Recovery, April 20-23, Tulsa, Oklahoma.

[82] Alagic, E. (2010) *Combination of low salinity water flooding with surfactant injection - A new hybrid EOR process*. PhD Dissertation University of Bergen.